A Genome-Wide Regulatory Framework Identifies Maize *Pericarp Color1* Controlled Genes[C][W]

Kengo Morohashi,[a,b] María Isabel Casas,[b,c] Maria Lorena Falcone Ferreyra,[d] María Katherine Mejía-Guerra,[b,c]
Lucille Pourcel,[e] Alper Yilmaz,[b,1] Antje Feller,[f] Bruna Carvalho,[b] Julia Emiliani,[d] Eduardo Rodriguez,[g]
Silvina Pellegrinet,[h] Michael McMullen,[i,j] Paula Casati,[d] and Erich Grotewold[a,b,2]

[a] Department of Molecular Genetics, The Ohio State University, Columbus, Ohio 43210
[b] Center for Applied Plant Sciences, The Ohio State University, Columbus, Ohio 43210
[c] Molecular, Cellular, and Developmental Biology Program, The Ohio State University, Columbus, Ohio 43210
[d] Centro de Estudios Fotosintéticos y Bioquímicos, Universidad Nacional de Rosario, Santa Fe S2002LRK, Argentina
[e] Department of Botany and Plant Biology, University of Geneva, Geneva 1211, Switzerland
[f] Department of Food Quality and Nutrition, Instituto Agrario San Michele all'Adige, 38010 San Michele all'Adige, Italy
[g] Instituto de Biología Molecular y Celular de Rosario, Rosario, Santa Fe S2002LRK, Argentina
[h] Instituto de Química, Rosario, Santa Fe S2002LRK, Argentina
[i] Plant Genetics Research Unit, U.S. Department of Agriculture–Agricultural Research Service, University of Missouri, Columbia, Missouri 65211
[j] Division of Plant Sciences, University of Missouri, Columbia, Missouri 65211

Pericarp Color1 (*P1*) encodes an R2R3-MYB transcription factor responsible for the accumulation of insecticidal flavones in maize (*Zea mays*) silks and red phlobaphene pigments in pericarps and other floral tissues, which makes *P1* an important visual marker. Using genome-wide expression analyses (RNA sequencing) in pericarps and silks of plants with contrasting *P1* alleles combined with chromatin immunoprecipitation coupled with high-throughput sequencing, we show here that the regulatory functions of *P1* are much broader than the activation of genes corresponding to enzymes in a branch of flavonoid biosynthesis. *P1* modulates the expression of several thousand genes, and ~1500 of them were identified as putative direct targets of *P1*. Among them, we identified *F2H1*, corresponding to a P450 enzyme that converts naringenin into 2-hydroxynaringenin, a key branch point in the *P1*-controlled pathway and the first step in the formation of insecticidal *C*-glycosyl flavones. Unexpectedly, the binding of P1 to gene regulatory regions can result in both gene activation and repression. Our results indicate that *P1* is the major regulator for a set of genes involved in flavonoid biosynthesis and a minor modulator of the expression of a much larger gene set that includes genes involved in primary metabolism and production of other specialized compounds.
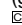
INTRODUCTION

Maize (*Zea mays*) kernel pigmentation was central to elucidating fundamental genetic principles, including correlated traits (Emerson, 1911), variegation (Emerson, 1917), allelic diversity (Anderson, 1924), transposable elements (McClintock, 1949, 1950), and in the original discovery of Mendel's laws and their rediscovery at the beginning of the 20th century (Mendel, 1950; Coe, 2001). Carotenoids and indole-derived compounds can color the maize caryopsis yellow or orange, respectively (Buckner
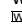
et al., 1990; Wright et al., 1992), and flavonoid pigments provide the red/purple pigmentation characteristic of "Indian maize." Among the flavonoid pigments, red, purple, or blue anthocyanins are ubiquitously distributed in the flowering plants and furnish one of the best-described plant biosynthetic pathways (Grotewold, 2006). In addition, the maize seed also accumulates brick-red phlobaphene pigments that result from polymerization of flavan-4-ols (Styles and Ceska, 1975, 1977, 1989), first identified in sorghum (*Sorghum bicolor*; Bate-Smith, 1969) and also present in wheat (*Triticum aestivum*), where they participate in the control of preharvest germination (Flintham, 2000). In maize, the phlobaphene pigments accumulate most conspicuously in floral organs, including the cob glumes and the pericarp. The pericarp is the outermost coat of the kernel, a 5- to 22-cell-layer-thick maternal tissue corresponding to the transformed ovary wall (Kiesselbach, 1980). The pericarp serves as the first barrier to insects and pathogens (Byrne et al., 1996b; Bily et al., 2003); it is the most important factor for the quality of sweet maize (Tracy and Galinat, 1987) and plays a key role as a moisture barrier, essential in popcorn (Tandjung et al., 2005). Following a period of cell expansion, the central cells in the pericarp start

collapsing in a process that starts at the crown around 10 d after pollination (DAP), spreading down the sides of the kernel. Adjusting to the expanding endosperm and starting around 20 DAP, inner pericarp cells collapse, while outer cells elongate with significant thickening of their cell walls (Garcia-Lara et al., 2004), resulting in a strong protective coat in the mature kernel (Tracy and Galinat, 1987). The formation of the phlobaphene pigments follows pericarp developmental changes, starting to accumulate in the crown 17 to 20 DAP, spreading down the sides of the kernel and giving a fully pigmented kernel by 30 to 35 DAP.

Phlobaphenes result from the polymerization of the 3-deoxyflavonoids luteoforol or apiforol (Figure 1), and their accumulation is controlled by the product of the *Pericarp Color1* (*P1*) locus (Styles and Ceska, 1975), encoding an R2R3-MYB transcription factor (Grotewold et al., 1994). Alleles of *P1* can pigment red the pericarp and the cob glumes (*P1-rr*, for red pericarp and red cob), only the cob glumes (*P1-wr*, for white pericarp and red cob), or neither one (*P1-ww*, for white pericarp and white cob). In some maize inbred lines, a segmental gene duplication resulted in the generation of a second copy of the gene, *P2*. In *P1-rr*, *P1* is primarily expressed in pericarp, cob glumes, and silks, but the expression of *P2* is mainly restricted to silks (Zhang et al., 2000).

P1 shares more than 80% identity in the R2R3-MYB domain with the anthocyanin regulator C1 (or its paralog PL1) (Grotewold et al., 1991b). In the presence of a member of the R/B family of basic helix-loop-helix proteins, C1/PL1 controls the expression of six known anthocyanin biosynthetic genes (*CHALCONE SYNTHASE* [*C2*], *CHALCONE ISOMERASE1* [*CHI1*], *FLAVONOID 3-HYDROXYLASE* [*F3H*], *DIHYDROFLAVONOL 4-REDUCTASE* [*A1*], *ANTHOCYANIDIN SYNTHASE*, and *UDP-GLUCOSYL TRANSFERASE*) (Goff et al., 1990; Roth et al., 1991; Tuerck and Fromm, 1994; Grotewold et al., 1998) and at least two genes implicated in vacuolar pigment sequestration (*GLUTATHIONE S-TRANSFERASE* and *MULTIDRUG RESISTANCE-ASSOCIATED PROTEIN3*) (Bodeau and Walbot, 1992; Goodman et al., 2004). By contrast, the P1 regulatory activity is independent of R/B, and the genes known to be required for the *P1*-dependent formation of 3-deoxyflavonoids are *C2*, *CHI1*, and *A1* (Grotewold et al., 1998).

P1 was also identified as a major quantitative trait locus (QTL) responsible for the accumulation of the *C*-glycosyl flavone maysin in maize silks, providing major resistance against the maize earworm, *Helicoverpa zea* (Byrne et al., 1996b). The metabolic steps resulting in the formation of the flavanone naringenin, a common precursor in the formation of the phlobaphenes and maysin (Figure 1), are understood, but most of the later steps in the respective pathways remain unknown, including the conversion of flavanones to flavones. Two different types of enzymes have evolved in plants to catalyze the conversion of naringenin or eriodictyol into apigenin or luteolin (Figure 1). Type I flavone synthases (FNSs) correspond to soluble 2-oxoglutarate-dependent enzymes found so far only in the Apiaceae, while type II FNS enzymes are more broadly distributed and correspond to P450s (Martens and Mithöfer, 2005). In some cereals, the formation of *C*-glycosyl flavones occurs by a different pathway that involves the initial hydroxylation of

flavanones to the 2-OH derivatives by a flavanone 2-hydroxylase (F2H), P450 enzymes with very high similarity to type II FNS (Brazier-Hicks et al., 2009). The 2-hydroxyflavanones (or its open ring isomer) serve as substrates for *C*-glycosyl transferases, which are then dehydrated (by a putative dehydratase) to result in the flavone-6-*C* or -8-*C*-glucosides (Brazier-Hicks et al., 2009).

In addition to flavones and 3-deoxyflavonoids, *P1* also controls the accumulation of chlorogenic (Bushman et al., 2002) and ferulic acids (Grotewold et al., 1998), suggesting a wider role of this R2R3-MYB regulator in the control of phenylpropanoid compounds than deduced from prior genetic analyses (Styles and Ceska, 1977).

P1 belongs to a distinct group of R2R3-MYB transcription factors that significantly expanded during the radiation of the grasses (Rabinowicz et al., 1999). The closest P1 relatives in *Arabidopsis thaliana* are PRODUCTION OF FLAVONOL GLYCOSIDES 1-3 (MYB11/12/111), responsible for the control of flavonol biosynthesis (Mehrtens et al., 2005; Stracke et al., 2007). Suggesting a functional conservation on how monocot and dicot plants control flavonols, *P1* was recently shown to directly regulate the maize flavonol synthase gene *FLS1*. The expression of *FLS1* and the consequent accumulation of flavonols is largely associated with the response to UV-B radiation (Ferreyra et al., 2010), with minimal flavonol levels present in maize pericarps. Besides *FLS1*, the only other gene confirmed as a P1 immediate direct target is *A1* (Ferreyra et al., 2010). Taken together, these findings suggest a function for P1 in controlling a broad range of phenolic compounds beyond the 3-deoxyflavonoids (Styles and Ceska, 1977).

To understand the function of P1 in controlling other aspects of phenolic metabolism and to establish how P1 fits in the maize gene regulatory network, we combined systems level approaches for the comprehensive identification of *P1*-regulated genes. We applied RNA sequencing (RNA-Seq) to identify genes that are differentially expressed in silks or pericarp tissues at different developmental stages, with contrasting *P1* genotypes (*P1-rr* versus *P1-ww*). We determined that *P1* significantly affected the expression of >1000 genes, some specific to pericarps or silks, and many shared between these tissues, reflecting their common origin. Pathways related to specialized metabolism, in particular phenylpropanoids, were identified as enriched major functional categories for the genes expressed higher in *P1-rr*, compared with *P1-ww*. To determine which of the genes differentially expressed between *P1-rr* and *P1-ww* pericarps were putative immediate (direct) targets of P1, we conducted chromatin immunoprecipitation coupled with high-throughput sequencing (ChIP-Seq) using P1 antibodies on pericarp chromatin. We identified several thousand genes as putative direct targets of P1, with a significant overlap to genes identified as controlled by *P1* in the RNA-Seq experiments. These included genes encoding novel enzymes that participate in the formation of 3-deoxyflavonoids, among them a previously unknown F2H. P1 has so far been known to function as a transcriptional activator (Grotewold et al., 1994; Tuerck and Fromm, 1994; Sainz et al., 1997). However, more than half of the *P1*-regulated genes, including several putative P1 direct targets, were lower in *P1-rr*, compared with *P1-ww*, suggesting that this regulator can also
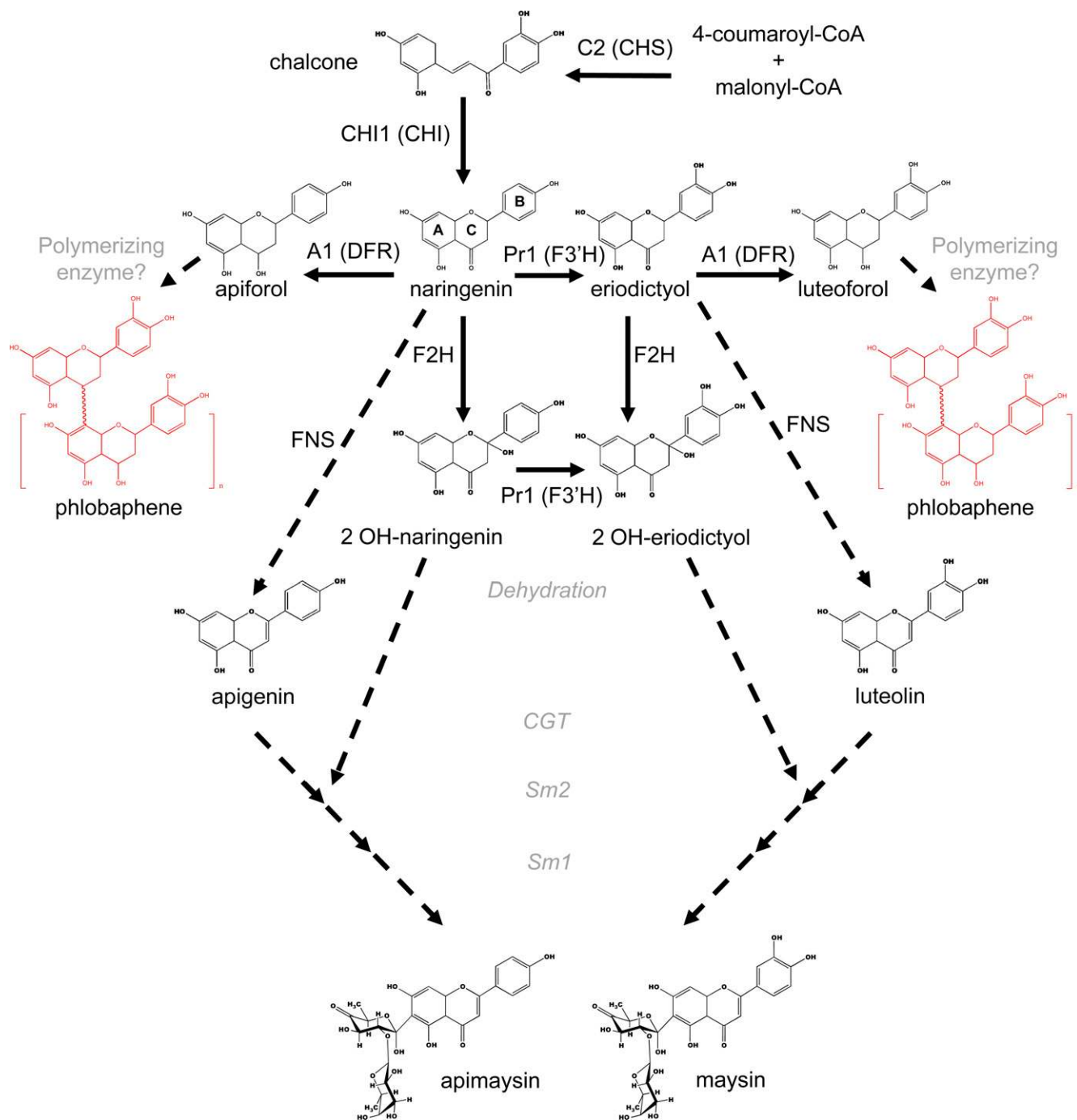
Figure 1. Maize 3-Deoxyflavonoid and Flavone Biosynthetic Pathways.

The condensation reaction between *p*-coumaroyl-CoA and malonyl-CoA, the first committed step in flavonoid formation, is catalyzed by chalcone synthase (*CHS*), resulting in naringenin chalcone (chalcone). This chalcone is converted to the flavanone naringenin by chalcone isomerase. Naringenin, the branching point of the pathway, is converted to apiforol (flavan-4-ol) by a dihydroflavonol reductase (DFR) to apigenin (flavone) by action of a F2H followed by a dehydration step (see Supplemental Figure 7C online). An FNS could also catalyze this step. Naringenin can also be converted to eriodictyol by a flavanone-3′-hydroxylase (F3′H) and serves as substrate for F2H/dehydration or FNS, forming the flavone luteolin. Dihydroflavonol reductase can also act on eriodictyol to generate the flavan-4-ol luteoforol. Apiforol and luteoforol polymerize to form the red phlobaphene pigments. The proposed steps for conversion of apigenin and luteolin into the *C*-glycosyl flavones apimaysin and maysin, respectively, involves at least three steps: glycosylation at C-6 by a CGT, followed by a rhamnosylation at *C*-1 of the Glc moiety possibly mediated by SM2, and finally a dehydration step mediated by SM1 (McMullen et al., 2004).

[See online article for color version of this figure.]

function as a transcriptional repressor. Taken together, this systems approach resulted in the discovery of maize flavonoid genes and provided information on the functions and regulatory mechanisms of *P1*.

RESULTS

Identification of *P1* Regulated Genes by RNA-Seq of *P1-rr* and *P1-ww* Developing Pericarps

To establish the overall regulatory function of the *P1* gene, we introduced by crossing a *P1-rr* allele (Grotewold et al., 1991a) into the A619 maize inbred, which harbors the recessive null *P1-ww* allele. A619 is negative in the silk browning reaction, accumulates negligible amounts of flavones in the silks (Bushman et al., 2002), and lacks *P2* function (Szalma et al., 2005). To capture important developmental changes associated with pericarp development, RNA-Seq experiments were performed on mRNA obtained from *P1-rr*^{A619} and *P1-ww*^{A619} pericarps (referred to from here on as *P1-rr* and *P1-ww*) at 14 and 25 DAP (see Supplemental Figure 1 online). High-throughput sequencing using the Illumina platform resulted in the generation of ~20 million high quality reads, from which ~90% aligned to the recently completed maize genome sequence (release 5b.60) (Schnable et al., 2009), corresponding to ~5 million reads for each one of the four samples (see Supplemental Table 1 online). The aligned reads were used to calculate the relative abundance of transcripts as the expected number of fragments per kilobase of transcript sequence per million base pairs sequenced (FPKM) (Trapnell et al., 2010).

First, we evaluated whether genes were significantly expressed (P < 0.05 based on a negative binomial model distribution; see Methods). This resulted in a total of 25,716 gene models represented in maize pericarp reads (combining 14 and 25 DAP), suggesting that ~65% or more of all the maize genes are transcribed in this tissue (Figure 2A). Next, we investigated how many genes are affected by the *P1* genotype by comparing the relative abundance of transcripts obtained from *P1-rr* and *P1-ww* pericarps using TopHat (Trapnell et al., 2009) with a cutoff P value of <0.02 and a false discovery rate (FDR) of <0.15 (see Methods). Based on these analyses, we determined that *P1* affects the steady state mRNA levels of 3202 genes. From these, 1346 show higher expression in *P1-rr*, compared with *P1-ww*, while 2019 show increased mRNA accumulation in the absence of *P1* function (Figure 2B). These results were unexpected, given our prior knowledge of *P1* function, for two main reasons. First, they suggest that *P1* has a much wider (direct or indirect) effect on gene expression than anticipated from the *p1* mutant phenotypes; second, they suggest that *P1* negatively (directly or indirectly) represses mRNA accumulation for a similar number of genes as it appears to activate. To validate the expression differences observed by RNA-Seq between *P1-rr* and *P1-ww* pericarps, we performed quantitative RT-PCR (qRT-PCR) on 18 differentially expressed genes (see Supplemental Data Set 1 online). We determined that in 16/18 cases, mRNA accumulation differences identified by RNA-Seq were also observed by qRT-PCR (see Supplemental Figure 2 online).

P1 Controls Overlapping yet Distinct Gene Sets in Maize Silks and Pericarps

Similarly as done for pericarps, we performed RNA-Seq on *P1-rr* and *P1-ww* unfertilized silks obtained promptly (<72 h) after emergence. This resulted in the generation of ~14 million high quality reads, corresponding to ~7 million reads for each sample (see Supplemental Table 1 online), from which 76% aligned to the maize genome. Applying similar criteria as above, we identified 24,431 gene models expressed in silks (Figure 2A), suggesting that at least ~62% of all the maize genes are transcribed in this tissue. For qRT-PCR validation, we selected 18 genes with higher expression in both *P1-rr* pericarps and silks (see Supplemental Data Set 1 online) and determined that 12 were expressed at significantly (P < 0.01, two-sided *t* test) higher levels in *P1-rr* silks compared with *P1-ww* silks (see Supplemental Figure 2 online).

The overall distribution of gene expression between pericarp and silk tissues is very similar and also very similar to genome-wide expression patterns established for maize root, shoot, and leaf tissues (Eveland et al., 2010) (see Supplemental Figure 3 online). As anticipated, given that silks and pericarps have the same developmental origin, the ovary wall (Kiesselbach, 1980; Huang and Sheridan, 1994), the patterns of gene expression are more similar between pericarps and silks than with other plant organs (root, shoot, or leaf), with the difference in *P1* genotype influencing gene expression patterns to a lesser extent than the origin of the tissue (see Supplemental Figure 3B online).

The steady state levels of a very large number (2363) of genes were affected by *P1* in silks, with 1223 mRNAs accumulating at higher level in *P1-rr*, compared with *P1-ww*, and 976 vice versa (Figure 2B). Interestingly, while a significant number of genes were affected in at least one pericarp sample as well as in silks (47 + 36 + 35 = 118 higher in *P1-rr* and 48 + 8 + 49 = 105 higher in *P1-ww*; Figure 2B), the vast majority of the genes affected by the presence of *P1* were different between these two tissues.

A detailed functional characterization of the genes belonging to the various groups, such as specific to the pericarp or to the silks, up- or downregulated by *P1* in a specific tissue (see Supplemental Data Set 1 online), revealed a number of striking patterns. For example, genes expressed at a higher level in 14-DAP *P1-rr* pericarps, compared with *P1-ww*, are significantly enriched in phenylpropanoid metabolism (P = 2.57 × 10^{-3}) but also in carbohydrate degradation and the cytosolic branch of glycolysis (P = 2.77 × 10^{-3} and P = 5.73 × 10^{-3}, respectively). By contrast, differentially expressed gene sets in 25-DAP pericarps include some implicated in lipid metabolism (in particular triacylglicerides), cellular organization, and RNA binding (see Supplemental Data Set 1 online). Genes activated by P1 in both 14 and 25 DAP are very significantly enriched in flavonoid biosynthesis (P = 9.9 × 10^{-9}) and the tricarboxylic acid cycle (P = 1.04 × 10^{-8}) functions. This may reflect the increased levels of malonyl-CoA (derived from lipid metabolism) and coumaroyl-CoA (derived from Phe) necessary for flavonoid formation (Figure 1) or may reveal other unexpected links between primary and secondary metabolism. Genes controlled by *P1* in silks are primarily enriched in P450s as well as in photosynthesis genes (see Supplemental Data Set 1 online). The overlap of the P1-induced
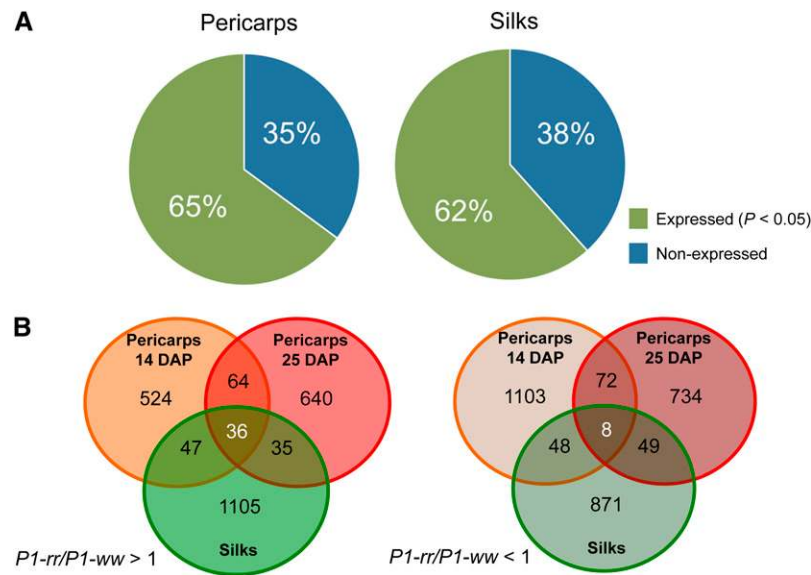
Figure 2. Pericarp and Silk Gene Expression Patterns.

(A) Ratios of expressed and nonexpressed genes in pericarps (left) and silks (right). Red or blue colors indicate expressed or nonexpressed genes, respectively.

(B) Venn diagrams summarizing the number of differentially expressed genes contrasting *P1-rr* and *P1-ww* pericarps (14 and 25 DAP) and silks. [See online article for color version of this figure.]

genes in pericarp (14 and 25 DAP) and silks (36 genes in total; Figure 2B) is significantly enriched in transcripts for enzymes in flavonoid biosynthesis, UDP-glucosyl and glucoronyl transferases, and the synthesis of cell wall precursors, primarily phenolics (see Supplemental Data Set 1 online). These results suggest that P1 plays a significant (direct or indirect) role in modulating carbon metabolism at specific stages of pericarp development, in addition to the expected participation in the control of phenylpropanoids. The biological processes associated with the genes repressed by P1 are completely different from those that P1 activates and are significantly enriched in cellulose biosynthetic genes and cell wall proteins, as well as in various signaling molecules (see Supplemental Data Set 1 online). One possible explanation for these results is that the need for cellulose biosynthesis is less acute in the presence of the high levels of phenolics specified by *P1* in *P1-rr* pericarps.

Also noteworthy was the finding that *P1* controls the expression of a significant number (378) of genes encoding transcription factors (see Supplemental Figure 4A online). Twenty of these transcription factor genes overlapped between 14- and 25-DAP pericarp comparisons, while none was represented in all three samples. Among those that *P1* controlled in the pericarp, several showed higher expression at 14 DAP with a decrease at 25 DAP. The regulatory genes that showed this behavior included *MYB95* (previously known as *MYB-IF25*; Dias et al., 2003), a gene with high similarity to *P1*, which was proposed to control the accumulation of phenylpropanoids (Dias and Grotewold, 2003). Transcription factors are generally assumed to express at very low levels. However, our analysis of the levels of mRNA accumulation for transcription factors expressed in pericarps indicates that the median of transcription

factor accumulation (see Supplemental Figure 4D online) is not significantly different from the median of expression for all genes expressed in pericarps (see Supplemental Figure 3A online). However, *P1* is expressed significantly below the median (see Supplemental Figure 4D online).

Control of a Discrete Gene Set by *P1* in Pericarps and Silks

In previous sections, we focused primarily on genes that were affected by *P1* in either pericarps or silks. However, a total of 72 genes that were very significantly (P = 1.08 × 10^{-27}, Fisher's exact test) differentially expressed between *P1-rr* and *P1-ww* in both pericarps and silks were also identified. These include the 36 genes expressed significantly higher in *P1-rr* pericarps (14 and 25 DAP) and silks, the eight genes expressed in all three tissues at a lower level in *P1-rr* (Figure 2B), and an interesting group of genes that showed opposite expression differences between any two of the three samples.

This set of 72 genes was subjected to K-means clustering, and a heat map displaying the eight clusters is shown (Figure 3). Genes in these eight clusters show very different expression patterns, when comparing how they respond to the P1 genotype in each of the three samples (see Supplemental Figure 5 online). Flavonoid biosynthetic genes are highly represented in clusters K1 and K2, corresponding to genes that are overall expressed at a much higher levels in all *P1-rr* samples, compared with *P1-ww* (see Supplemental Figure 5 online). These include *CHI1* and *A1*, two flavonoid biosynthetic genes previously shown to be controlled by *P1* (Grotewold et al., 1998). Interestingly, *C2* is also expressed at a very high level in *P1-rr* tissues, compared with *P1-ww*, but was not included in the 72 genes set because
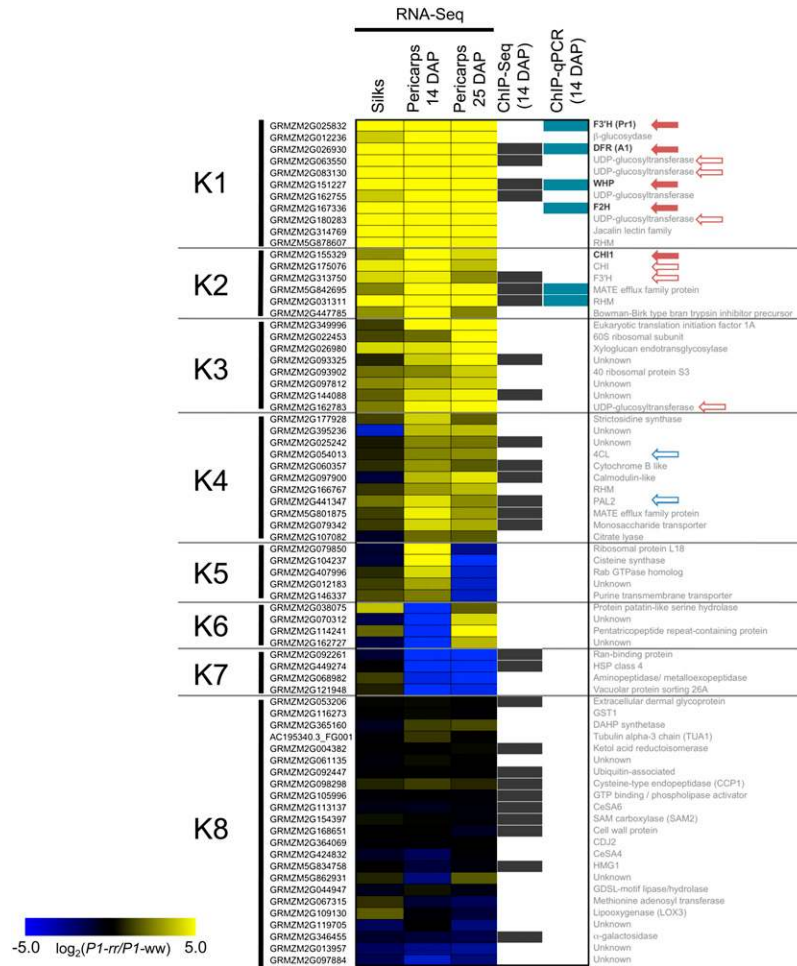
Figure 3. Cluster Analysis of *P1*-Controlled Genes in Silks and Pericarps.

Genes differentially expressed between *P1-rr* and *P1-ww* pericarps (14 and 25 DAP) and silks were grouped into eight clusters (K1 to K8) to represent the different patterns observed. Black boxes indicate genes identified as putative direct targets of P1 by ChIP-Seq, and blue boxes indicate genes identified as putative direct targets of P1 by ChIP-qPCR. In addition, gene names shown in bold and indicated by red (closed) arrows correspond to ones previously described as involved in the flavonoid pathway. Genes indicated with red or blue (open) arrows correspond to gene models predicted to participate in flavonoid and phenylpropanoid biosynthesis, respectively.

a significant expression in *P1-ww* silks resulted in a P value and FDR that were above the threshold (P < 0.02 and FDR < 0.15). Nevertheless, *C2* expression was 16 times higher in *P1-rr* silks, compared with *P1-ww*, and 354 and 69 for 14- and 25-DAP pericarps, respectively. The 72 genes also include a putative *CHI* (GRMZM2G175076), as well as *WHP1* (GRMZM2G151227), a second maize chalcone synthase gene (Franken et al., 1991), which was previously shown to be controlled by *P1* in silks (Meyer et al., 2007).

To better understand the regulation of these paralogs, we cloned the regions corresponding to 423 bp upstream of the *WHP1* and 1249 bp upstream of the *C2* transcription start sites (TSSs) in a vector harboring the luciferase gene reporter (pWHP:Luc and pC2:Luc, respectively). By transient expression analyses, we determined that in maize protoplasts, *P1* activates both promoters (see Supplemental Figures 6B and 6C online). However, C1+R, corresponding to regulators of anthocyanin

biosynthesis that very robustly activate when together *A1* and *C2*, are very inefficient at activating pWHP:Luc (see Supplemental Figure 6C online). *A1** corresponds to a putative paralog of *A1* (Bernhardt et al., 1998). Our RNA-Seq results show that, in contrast with *A1*, which expresses at high levels in all the *P1-rr* tissues, *A1** is primarily expressed in 14-DAP pericarps and silks (see Supplemental Figure 6A online). As described above for *C2* and *WHP1*, we assayed by transient activation the regulation of pA1*:Luc. Similarly as we found for *WHP1*, *A1** is activated by P1 with almost no effect by C1+R (see Supplemental Figures 6B and 6C online). These results suggest that the nonredundant function of these two paralogous pairs (*C2-WHP* and *A1-A1**) is in large part a consequence of being differentially controlled by these two sets of flavonoid transcription factors. Moreover, they suggest that previous findings showing P1 activates *A1* transcription at lower levels than C1+R (Grotewold et al., 1994; Sainz et al., 1997; Hernandez et al., 2004) reflect a preference of

P1 for other promoters, rather than *P1* being an inefficient transcriptional activator. We further demonstrated using in vitro protein-DNA binding assays that P1 binds to at least two *cis*-regulatory elements in the *WHP1* promoter (see Supplemental Figure 6D online). These two sites, harboring the CCAACC motif, fit well the previously identified P1 DNA binding consensus (Grotewold et al., 1994).

Cluster K3 corresponds to genes induced by *P1* much more strongly in pericarps than in silks (Figure 3; see Supplemental Figure 5 online). With the exception of a putative UDP-glucosyltransferase and several genes of unknown function, K3 is enriched in genes involved in translation, suggesting that perhaps the increased accumulation of metabolic enzymes induced by *P1* requires also the expression of rate-limiting components of the translational machinery.

Similar to K3, cluster K4 harbors genes induced by *P1* primarily in the pericarp. This category contains two phenylpropanoid genes, a 4-coumarate-CoA-ligase (*4CL*; GRMZM2G054013) and a *PAL* (GRMZM2G441347), possibly *PAL2* based on its location in chromosome 2. This *PAL* gene likely correspond to L77912/AF204900, previously identified as induced by *P1* by the ectopic-inducible expression of this transcription factor in Black Mexican Sweet cells (Bruce et al., 2000). The steady state mRNA accumulation of *PAL2* was determined to be induced by *P1* in 14-DAP pericarps and silks by qRT-PCR, although this induction was not deemed to be statistically significant ($P = 0.085$ and 0.107, respectively) as a consequence of the high variability of mRNA levels observed (see Supplemental Figure 2 online).

Clusters K5 to 7 are interesting as they contain genes that display opposite regulation by P1 in at least two of the three samples (Figure 3; see Supplemental Figure 5 online). K5 genes are repressed by *P1* in 25 DAP pericarps, yet induced at 14 DAP. Most of the K5 genes are also induced by *P1* in silks. Opposite to K5, K6 contains genes that are activated by *P1* in 25 DAP, yet repressed in 14 DAP pericarps. K7 contains genes that are only activated by *P1* in silks, but repressed in pericarps at both developmental stages. These clusters include genes with a diverse range of functions (Figure 3).

Finally, cluster K8 depicts genes that are significantly, yet very weakly, modulated by *P1* (see Supplemental Figure 5 online). Similar to K5 to 7, genes in this cluster do not show an obvious enrichment in any functional category, although they contain two cellulose synthases (CesA) and a Pro-rich glycoprotein likely localized to the cell wall.

P1-Controlled Genes Fill Gaps in the Maize Flavonoid Biosynthetic Pathway

The analysis of clusters K1 and K2 also resulted in the identification of several novel genes with a possible role in flavonoid metabolism (Figure 3, open red arrows). Among them, we identified GRMZM2G167336 as accumulating at significantly higher levels in *P1-rr* pericarps and silks (Figure 3; see Supplemental Figure 2 online) and which shows high identity in the coding region with type II FNSs, characterized from sorghum (Du et al., 2010b), rice (*Oryza sativa*; Du et al., 2010a) (89 and 74%, respectively), and other plants (Martens and Mithöfer, 2005). To

determine the possible FNS/F2H activity for the product of this gene, we cloned the full-length GRMZM2G167336 open reading frame in the pGZ25 (a modified version of YEplac112; Gietz and Sugino, 1988) yeast expression vector under the constitutive glyceraldehyde-3-phosphate dehydrogenase promoter and transformed the WAT11 yeast strain (Pompon et al., 1996) expressing the *Arabidopsis* ATR1 P450 reductase. Transformed WAT11 yeast cells were supplied with naringenin or eriodictyol, and HPLC analyses showed that cell extracts and supernatants accumulated the corresponding flavones (apigenin and luteolin, respectively) (Figure 4A, F2H1), which were not present in a WAT11 strain harboring an empty pGZ25 plasmid (Figure 4A, empty vector). Yeast was previously described as harboring a dehydratase activity capable of converting 2-hydroxyflavanones into the corresponding flavones (Zhang et al., 2007). Thus, we performed liquid chromatography–mass spectrometry (LC-MS) experiments to detect whether traces of 2-hydroxynaringenin were detectable after incubating the transformed yeast cells with naringenin. Because 2-hydroxynaringenin is not commercially available, we chemically synthesized it from apigenin (see Methods). Using the chemically synthesized 2-hydroxynaringenin, we established by LC-MS that yeast cells harboring putative F2H1 accumulate low, yet detectable levels of 2-hydroxynaringenin (see Supplemental Figures 7A and 7B online). In addition, when cells were supplemented with eriodictyol, we identified the formation of 2-hydroxyeriodictyol by LC-MS analyses scanning for a precursor ion of mass-to-charge ratio of 305 (data not shown). Taken together, these results demonstrate that GRMZM2G167336 corresponds to *F2H1*, encoding an enzyme capable of converting naringenin or eriodictyol into the corresponding 2-hydroxy derivatives (Figure 1), a key missing step in the formation of maysin and other maize insecticidal flavones.

ChIP-Seq Identifies *P1* Direct Target Genes

To establish which of the genes differentially expressed between *P1-rr* and *P1-ww* tissues are directly regulated by P1, we performed ChIP-Seq experiments with P1 polyclonal antibodies (αP1[344]) that recognize the nonconserved C-terminal region of P1 (Ferreyra et al., 2010). We determined by immunoblot analyses of pericarp nuclear proteins with αP1[344] that the P1 protein accumulates at significantly higher levels in 14-DAP pericarps compared with 25 DAP (see Supplemental Figure 8 online). Thus, ChIP-Seq experiments were conducted on chromatin extracted from the same 14-DAP pericarp samples as used for RNA-Seq. The very high content of flavonoids and other phenolic compounds present in particular in *P1-rr* pericarps significantly interfered with conventional ChIP approaches (Morohashi and Grotewold, 2009; Morohashi et al., 2009; Xie et al., 2010), compelling us to develop changes to the method that might be suited for other plant tissues rich in phenolics (see Methods). As a positive control, we used the *A1* gene that we previously showed to be directly regulated by P1 (Ferreyra et al., 2010). We conducted ChIP-Seq on two biological replicates for each 14-DAP *P1-rr* and *P1-ww* pericarp, using the Illumina platform (50- to 75-nucleotide-long single-end reads) with indexed adaptors that allowed multiplexing (see Methods). A total of ~10 million reads were sequenced, out of which 2.4
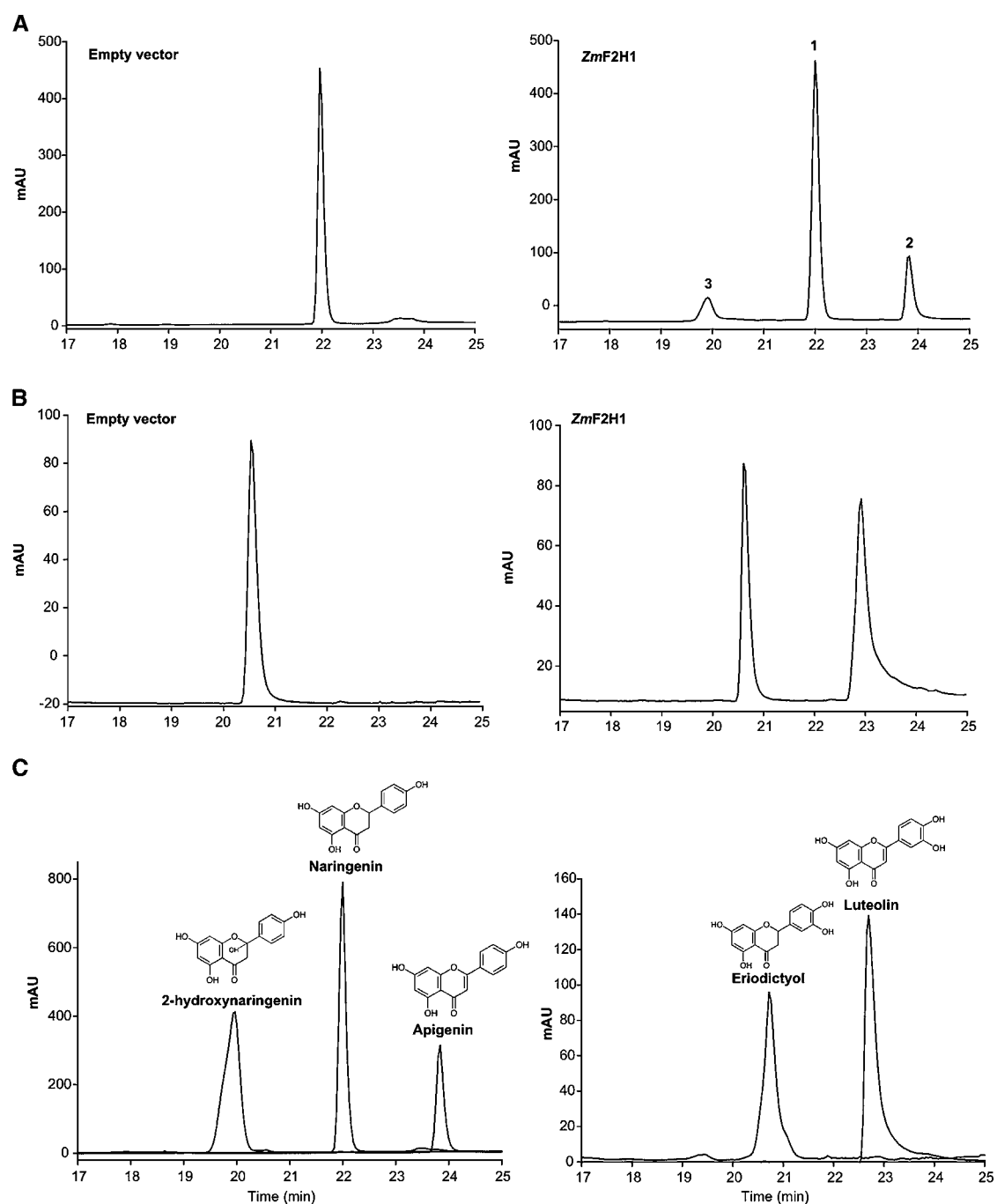
Figure 4. HPLC Profiles of WAT11 Yeast Cells Expressing Maize F2H1.

(A) Yeast cultures supplemented with naringenin (peak 1) in the presence of empty vector (left) or F2H1 (right) showing apigenin production (peak 3). mAU, milli absorbance units.
(B) Yeast cultures were supplemented with eriodictyol to test production of luteolin by F2H1 (right). F2H1 expressed in yeast also produces 2-hydroxynaringenin (time = 19.8 min) using naringenin as a substrate.
(C) Authentic standards were used as controls.

million uniquely mapped to the maize genome (release 5b.60), a percentage that is comparable to those in other studies in animals, yeast, and plants (Kaufmann et al., 2009; Lefrançois et al., 2009; Niu et al., 2011). The P1 binding locations in the genome were predicted by MACS (Zhang et al., 2008) (P < 1 × 10^{-4}, based on a Poisson distribution comparing *P1-rr* and *P1-ww* ChIP-Seq) and represented ~35,000 different peaks (see Supplemental Table 2 online).

Before conducting additional analyses, we randomly selected regions identified as enriched in P1 from one (17 regions) or both (five regions) ChIP-Seq replicates and tested them by ChIP-PCR. This resulted in 19/22 (14/17 and 5/5) randomly selected peaks validated (see Supplemental Figure 9 and Supplemental Table 3 online). These results demonstrated that putative targets identified in both replicates provide a very conservative (but high certainty) estimate of the P1 direct targets. Taking the union of both experiments significantly increases the identified putative targets without greatly increasing false positive identification.

As a first step to analyze the genes bound by P1 in the ChIP-Seq experiments, we concentrated our analyses on genic regions, arbitrarily defined here as the genomic segment comprised by genes and associated 5 kb upstream of the TSS (or ATG if the TSS is not yet determined) and 5 kb downstream of the site corresponding to where the poly(A) was found. Thus, to every gene model in the maize genome, we added 10 kb, 5 kb upstream, and 5 kb downstream. As is the case for other plant transcription factors for which genome-wide location analyses (e.g., ChIP-Seq or ChIP-chip) were conducted (Lee et al., 2007; Morohashi and Grotewold, 2009; Kaufmann et al., 2010), a large number (63%) of P1 binding sites locate to intergenic regions (Figure 5A), 5 kb or more away from any annotated gene. However, a significant enrichment of *P1* binding sites was found in the 5 kb upstream regions (Figures 5A and 5B). Indeed, a detailed analysis of the specific regions to which P1 binds shows that there is a significant enrichment surrounding the TSS (Figure 5C), in line with results suggesting that for genes such as *A1* (Grotewold et al., 1994) and *C2* (see Supplemental Figure 6 online), short fragments immediately upstream of the TSS are sufficient to recapitulate P1 activation. These P1 DNA binding pattern in a bell shape around the TSS is similar to what has emerged from the analysis of the DNA binding for a large number of transcription factors in humans, as part of the ENCODE project (Birney et al., 2007).

Overlay of ChIP-Seq and RNA-Seq Reveals Activating and Repressive *P1* Functions

From the 5565 gene models that RNA-Seq revealed as differentially expressed between *P1-rr* and *P1-ww* tissues, ChIP-Seq identified 1586 genes as putative direct P1 targets, a statistically significant overlap (P = 7.3 × 10^{-5}, Fisher's exact test). This overlap is remarkable since there is in general a poor correlation between expression and in vivo binding experiments (Moreno-Risueño et al., 2010; Biggin, 2011), and our ChIP-Seq was conducted only on 14 DAP pericarps. However, if we compare the genes activated by *P1* in 14-DAP pericarps (741 genes;

Figure 6A, *P1-rr/P1-ww* > 1) and the ChIP-Seq results obtained from the same tissue (10,468 genes; Figure 6A), the number of genes in the overlap is not significantly different from just chance (Figure 6A). We found a similar situation with genes repressed by P1 in 14-DAP pericarps (1320 genes; Figure 6A, *P1-rr/P1-ww* < 1), although in this case the overlap (368 genes) with genes bound by P1 has better statistical support (P = 0.11; Figure 6A). These findings may suggest that in 14-DAP pericarps, P1 binds to, but does not control, genes that are controlled by this regulator in other tissues or developmental stages.

The overlap between ChIP-Seq and RNA-Seq is significantly larger in the set of 72 genes that shows regulation by P1 in all three samples (Figure 3). Indeed, out of the 72 genes in that set, 28 were also identified as P1 putative direct targets in the ChIP-Seq results (Figure 3, black bar at the right). ChIP-Seq identified putative *P1* targets that were present in all clusters except K5 and K6 (Figure 3), suggesting that genes in clusters K5 and 6 are controlled indirectly by P1.

To better understand how P1 functions as an activator and repressor of distinct sets of genes, we focused on those overlapping between the RNA-Seq and ChIP-Seq experiments conducted on 14-DAP pericarps (Figure 6A). When we analyzed the distribution of the position of the peaks obtained from ChIP-Seq, we found that P1 binding occurred in similar regions, regardless of whether P1 functioned as an activator (red line, Figure 6B) or a repressor (blue line, Figure 6B).

To identify possible *cis*-regulatory motifs that would be associated with regulation by P1, we extracted the sequences corresponding to the P1 binding peaks from the genes expressed higher in *P1-rr* 14 DAP pericarps (196 upregulated genes; Figure 6A) or those expressed higher in *P1-ww* (368 downregulated genes; Figure 6A). We applied the ab initio motif discovery tool MEME-ChIP (Machanick and Bailey, 2011) on each of the peak sets separately and selected the top motif identified for each peak set (see Supplemental Figure 10A online). Interestingly, the most significantly enriched motif consisted in both cases of a sequence overall characterized by the presence of repeats with the $(CXXC)_{6-8}$ sequence, where X corresponds to any nucleotide (see Supplemental Figure 10A online). This motif was present in 120/227 peaks in the upregulated set and in 72/471 peaks in the downregulated set, and for both gene sets, the position of the peaks harboring the motifs followed a distribution around the TSS very similar to Figure 5C (data not shown). Systematic evolution of ligands by exponential enrichment experiments demonstrated that P1 binds DNA in vitro with the $ACC^{T}/_{A}ACC$ preference (Grotewold et al., 1994; Williams and Grotewold, 1997), and *cis*-regulatory elements singularly fitting such consensus were shown to be important in the regulation of *A1* by P1 (Grotewold et al., 1994). Both of these motifs have in common the CxxC core. In contrast with the DNA sequence that P1 preferentially binds in vitro, the motif identified here does not show a preference for A or T between the C base pairs. Indeed, several other transcription factors have been shown to display significantly different DNA binding preferences in vivo and in vitro (Carr and Biggin, 1999; Yang et al., 2006; Rabinovich et al., 2008).

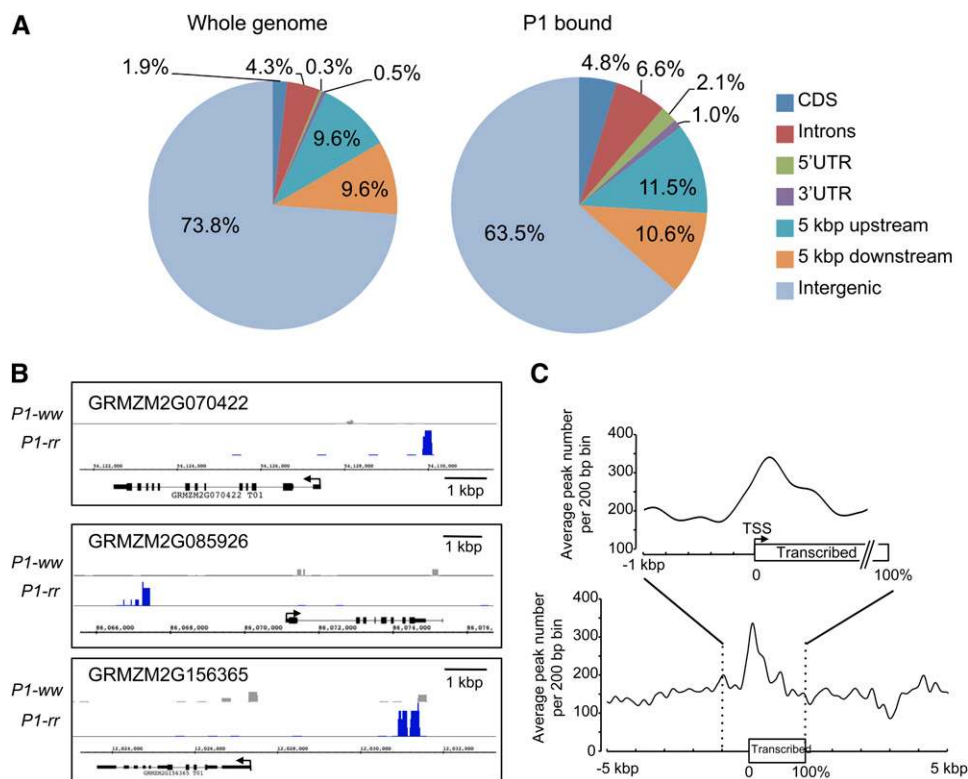Given the good understanding that we have of the DNA sequences that P1 recognizes in vitro (Grotewold et al., 1994;

Figure 5. Summary of P1 ChIP-Seq Results.

(A) Distribution of P1 binding regions (right) relative to the overall maize genome gene structure (left). For this analysis, the components of the genome were divided into intergenic (gray), 5 kb upstream (light blue), 5 kb downstream (orange), 5′ untranslated region (UTR) (green), 3′ untranslated region (purple), intron (red), and coding sequence (CDS) (dark blue) segments, as shown at the right of the graphs.

(B) Representative P1 binding peaks are shown by Integrated Genome Browser. For each gene model, the T01 splicing variant (maize genome version 5b.60) is shown. Large boxes indicate exons. TSS is indicated by an arrow. Aligned reads are indicated in gray (*P1-ww* 14 DAP) or blue (*P1-rr* 14 DAP).

(C) Distribution of average number of P1 binding peaks per 200-bp bin corresponding to the (−5000; +5000) region flanking the TSS (bottom), including transcribed regions. A magnification of this region is shown above.

Williams and Grotewold, 1997), we asked whether the genes regulated by P1 and harboring regulatory regions bound P1 in vivo were enriched for the presence of $CC^{T}/_{A}ACC$ sequences. Toward this, we separately analyzed the 227 and 471 peaks of the upregulated and downregulated genes, respectively (Figure 6A; see Supplemental Figure 10 online). We generated for each data set a background model consisting of 1000 permutations of the same number of genomic regions (227 for upregulated and 471 for downregulated) of identical length. We then analyzed the presence of DNA sequences fitting the P1 binding consensus and counted the number of appearances in the experimental set and in the 1000 simulated sets (see Supplemental Figure 10 online). For P1 upregulated genes, this sequence was present in 75 peaks, a very significant ($P = 1.68 \times 10^{-3}$) enrichment over the background model. For downregulated genes, P1 binding motifs were found in 155 peaks, again significantly ($P = 7.36 \times 10^{-5}$) higher than expected by chance. Taken together, these results indicate that, while there is an enrichment of canonical P1 binding motifs in the peaks identified from genome-wide location analyses, other DNA motifs $(CxxC)_{6-8}$ are preferentially enriched. Whether P1 is directly binding to the

$(CxxC)_{6-8}$ motif in vivo or whether this motif reflects a tethering of P1 through a cofactor remains to be established.

DISCUSSION

One hundred years of genetic studies have cemented the role of *P1* as the regulator of the phlobaphene pigments in the pericarp of maize (Anderson and Emerson, 1923). Subsequent studies revealed a role for *P1* in controlling other flavonoids, including insecticidal flavones (Byrne et al., 1996b) and flavonols, and identified a few genes directly regulated by *P1*, including *A1* and *FLS1* (Ferreyra et al., 2010). Distinct from C1 and R, P1 does not control anthocyanin biosynthesis (Grotewold et al., 1994), and genes controlled by P1, but not by C1/R, have yet to be identified. P1 has generally been considered a nice example for a transcription factor located low in a hierarchical gene regulatory network: *P1* appears to control just a few genes in a well-studied biosynthetic pathway, and *P1* mutants (e.g., *P1-ww*) are phenotypically indistinguishable from lines expressing *P1*, with the exception of the accumulation of phlobaphenes and other flavonoids in various floral tissues.
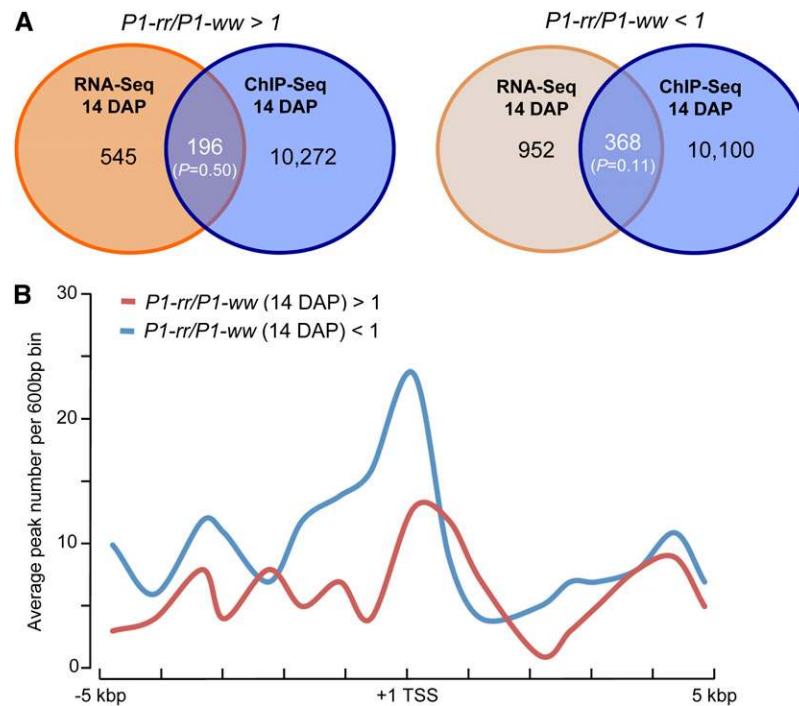
Figure 6. ChIP-Seq and RNA-Seq Comparison.

(A) Venn diagram representations that compare ChIP-Seq and RNA-Seq at 14 DAP. P values by Fisher's exact test are shown under gene numbers of intersections.

(B) Average number of P1 binding peaks per 600 bp corresponding either to 14-DAP *P1-rr/P1-ww* > 1 (red) or *P1-rr/P1-ww* < 1 (blue).

Indeed, most maize inbred lines lack pericarp *P1*-controlled pigments.

However, the results presented here suggest a significantly more complex situation, one that highlights a role of *P1* in the control of the expression of several thousands maize genes, many of them directly, as revealed by ChIP-Seq experiments conducted in pericarps with contrasting *P1* genotypes.

Distinctive Expression Patterns for Pericarps and Silks

The pericarp of the maize caryopsis originates from the fusion of three carpels, which form, prior to pollination, the ovary wall. During the upward growth, two of these carpels form an outgrowth that ultimately develops into the style, or silk (Kiesselbach, 1980). Thus, the pericarp and the silk have a common ontogeny. Not surprisingly, the gene expression patterns in these two maize organs are much more similar to each other than to leaves, roots, or stems (see Supplemental Figure 3 online). Only recently, and as part of an effort to develop a genome-wide atlas of maize gene expression during development, has the expression of genes in pericarps and silks been investigated using a microarray platform (Sekhon et al., 2011). This offered us an opportunity to compare gene expression results derived from microarray, with those obtained from RNA-Seq. As expected, both platforms show a significant overlap. However, RNA-Seq permitted us to identify 7642 additional genes expressed in the pericarp and 5988 more genes expressed in silks (see Supplemental Figure 11 online). These results highlight the higher

detection power of RNA-Seq over microarray-based technologies (Wang et al., 2009).

Previous studies suggested that the expression of *P1* in the pericarp is very low (Lechelt et al., 1989). Consistent with this, our results show that, when compared with other pericarp-expressed transcription factor genes, *P1* is expressed at levels below the median (FPKM ~8; see Supplemental Figure 4B online). In sharp contrast, and highlighting the efficacy of *P1* as a transcriptional activator, the direct target *A1* is expressed in pericarps in the top quartile. Indeed, in the presence of the *P1-rr* allele, the expression of *A1* (FPKM = 7228) is significantly stronger than the expression of the housekeeping genes *Actin1* or *Ubiquitin* (see Supplemental Figure 3 online), the latter in particular generally considered to be very strongly expressed (Christensen and Quail, 1996). This provides a good estimate that the amplification of expression provided by a regulator on its targets can be very variable, and as high as 1000-fold.

P1 Controlled Genes Fill a Key Step in the Biosynthesis of Insecticidal Flavones

Naringenin is a key intermediate in the formation of P1-regulated flavonoids (Figure 1). The conversion of flavanones (naringenin or eriodictyol) to flavones occurs by different mechanisms, depending on whether the product is the flavone aglycone (apigenin or luteolin) and the corresponding *O*- or *C*-glycosides (Brazier-Hicks et al., 2009). Apigenin or luteolin are normally present at low levels in pericarps because most of the pathway
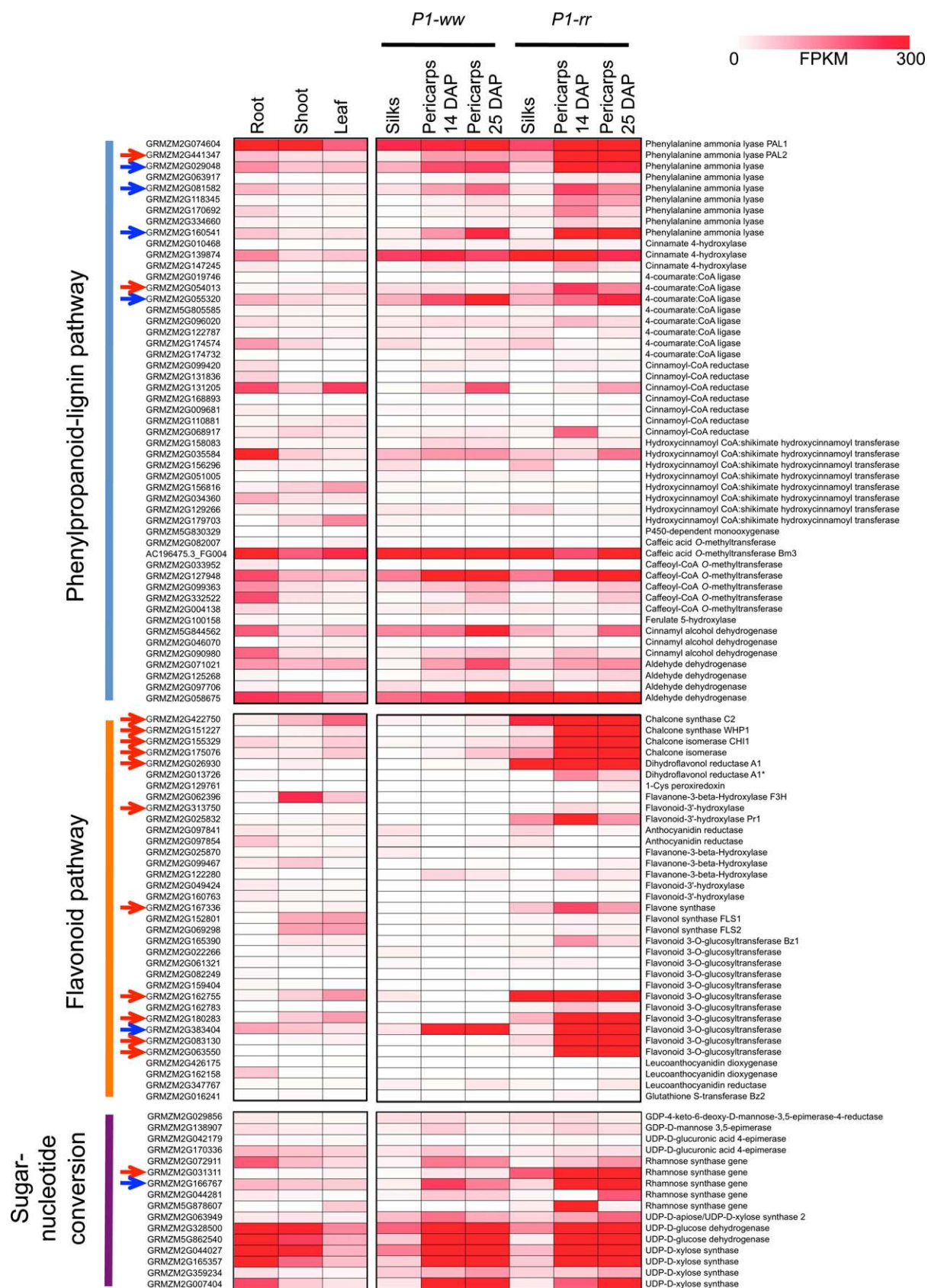
Figure 7. Expression Patterns of Maize Phenylpropanoid Genes.

is channeled toward the formation of flavan-4-ols (Styles and Ceska, 1977, 1989). However, *P1-rr a1* pericarps are brown (Meyers, 1927) and accumulate significant levels of *C*-glycosyl flavones (Styles and Ceska, 1989), suggesting the potential of this organ to form flavones. By contrast, *P1-rr* silks accumulate large quantities of *C*-glycosyl flavones (Waiss et al., 1979; Wiseman et al., 1993; Byrne et al., 1996a; McMullen et al., 2001), with little or no accumulation of apigenin or luteolin. We identified here a maize enzyme capable of converting naringenin or eriodictyol into the corresponding 2-hydroxyflavanones (Figure 4), which are then expected to serve as substrates for *C*-glycosylation, followed by dehydration and formation of the corresponding *C*-glycosyl flavones (Figure 1). Our RNA-Seq results identified several candidate glycosyltransferases that might provide the next step in the pathway, including some with significant similarity to rice CGT, a UDP-glucosyltransferase that uses 2-hydroxyflavanones as flavonoid acceptors (see Supplemental Figure 12 and Supplemental Data Set 3 online). However, previous studies identified trace amounts of luteolin specifically in the *sm2* mutant, leading to the suggestion that luteolin is one of the *C*-glycosylation substrates (McMullen et al., 2004). This prompts the question of whether maize encodes, in addition to F2H1, a bona fide FNS, an enzyme capable of converting naringenin into apigenin, without the 2-hydroxy-flavanone intermediate. In soybean (*Glycine max*), a second CYP450 FNS II (CYP93B16; see Supplemental Figure 7D and Supplemental Data Set 4 online) was implicated in the biosynthesis of flavones (and the corresponding *O*-glycosides) by catalyzing the direct desaturation of flavanones to flavones (Fliegmann et al., 2010). It is possible that a similar situation occurs in maize, which harbors two genes (GRMZM2G407650, annotated as CYP93G6, and GRMZM2G148441, annotated as CYP93G7) with higher identity to CYP93G1 than to the CYP93G2 candidates for the F2H activity. However, GRMZM2G407650 and GRMZM2G148441 are expressed at very low levels and are not induced by *P1* in pericarps and silks, as evidenced by the RNA-Seq results, suggesting that, if the direct reaction from naringenin to apigenin (or eriodictyol to luteolin) takes place, it is unlikely controlled by P1.

Contribution of *P1* to Phenylpropanoid Gene Regulation

In addition to flavonoids, the ectopic expression of *P1* in maize cultured cells showed a role for this MYB transcription factor in the regulation of ferulic and chlorogenic acids (Grotewold et al., 1998), consistent with the role of *P1* as a major QTL controlling chlorogenic acid accumulation in silks (Szalma et al., 2005). Moreover, the ectopic-inducible expression of *P1* in Black Mexican Sweet cells resulted in the induction of *PAL* and *CAD* genes (Bruce et al., 2000). To understand the role of *P1* in the control of phenolics in pericarps and silks, we generated a comprehensive list of phenylpropanoid

genes, based on previously characterized genes, available from literature (Penning et al., 2009) and our own analysis of the maize genome (see Methods). We analyzed the expression of this set of 101 phenylpropanoid genes (see Supplemental Data Set 2 online) for expression in *P1-rr* and *P1-ww* 14- and 25-DAP pericarps and silks, as well as in public data sets (Eveland et al., 2010) containing RNA-Seq results from B73 roots, shoots, and leaves (Figure 7). The analysis revealed that several phenylpropanoid genes are expressed exclusively (or at much higher levels) in pericarps, irrespective of the *P1* genotype (blue arrows, Figure 7), suggesting that this tissue might have a dedicated set of enzymes to synthesize phenolic compounds. The phenylpropanoid genes that are affected the most by *P1* correspond primarily to flavonoid genes, with only a few belonging to the core phenylpropanoid pathway, including GRMZM2G054013, encoding a *4CL*, and three *PAL* genes (GRMZM2G441347, GRZM2G334660, and GRMZM2G170692; Figure 7; see Supplemental Figure 2 online). *PAL1* is expressed at high levels in all tissues tested (Figure 7), and *PAL2* is controlled by *P1* in both pericarp and silks. Distinct from *PAL1*, *PAL2* is expressed at low levels in shoot and leaf tissues (Figure 7). GRMZM2G170692 encodes another *PAL* gene located in chromosome 5 and is significantly induced by *P1* in both pericarps and silks (see Supplemental Figure 2 online). None of the three *CAD* genes identified in the genome showed a significantly higher expression in *P1-rr* tissues compared with *P1-ww*.

How does *P1* control the accumulation of chlorogenic acid? In *Arabidopsis*, chlorogenic acid is formed by the action of CYP98A3 (C3H = *p*-coumarate-3-hydroxylase, also known as *p*-coumaroyl shikimate/quinate 3′-hydroxylase or C3′H) from the 5-*O*-quinate ester of *p*-coumaric acid (Schoch et al., 2001). We identified putative candidate genes for CYP98A3 from the maize genome and determined that one of them (GRMZM2G138074) is induced two- to threefold in 14- and 25-DAP pericarps by the presence of *P1* (see Supplemental Data Set 1 online), but not in silks; hence, it is not present in the 72 genes displayed in Figure 3. Most interestingly, GRMZM2G138074 was also identified in the ChIP-Seq experiments as a P1 direct target (see Supplemental Data Set 1 online) and validated by ChIP-qPCR (see Supplemental Figure 13 online). This *C3H* gene corresponds to a candidate QTL for resistance to Mediterranean Maize Borer (Ordas et al., 2010). Moreover, QTLs for chlorogenic acid levels were reported in multiple populations in the bin and neighbors to *C3H* (chromosome 3) (Bushman et al., 2002). In addition to C3H, chlorogenic acid biosynthesis would require enzymatic conversions performed by PAL, C4H, and 4CL, enzymes for which at least one family member is expressed at higher levels in *P1-rr*, compared with *P1-ww* tissues (Figure 7). These results demonstrate that *P1* is not a general regulator of phenylpropanoid biosynthesis but rather controls a specific set of genes required for the formation of flavonoid precursors and of some phenylpropanoids, such as chlorogenic acid.

Figure 7. (continued).

Heat map representation of the expression patterns of phenylpropanoid genes. Genes encoding candidate sugar nucleotide conversion enzymes are also included. RNA expression data were derived from the studies presented here (*P1-rr* and *P1-ww* pericarps and silks) or from publicly available data sets (root, shoot, and leaf) RNA-Seq results (Eveland et al., 2010).

P1 also regulates the expression of several genes (GRMZM2G166767, GRMZM2G031311, GRMZM2G044281, and GRMZM5G878607) annotated as rhamnose synthases (*RHM*). GRMZM2G031311 is also a direct target of P1, as evidenced by ChIP-Seq (Figure 3), in addition to being highly upregulated in *P1-rr* silks and pericarps (Figure 7). Regarding the other putative *RHM* genes, GRMZM2G044281 is highest expressed in *P1-rr* 25 DAP; GRMZM2G166767 is highly upregulated in *P1-rr* pericarps and GRMZM5G878607 in *P1-rr* 14 DAP and is not expressed at detectable levels in *P1-ww* silks (Figure 7). *RHM* convert UDP-Glc to UDP-Rha, and even though in bacteria this process is performed by independent enzymes (RmlB, RmlC, and RmlD), in plants, this process is performed by a bifunctional enzyme capable of both dehydrating and reducing UDP-Glc to UDP-Rha (Watt et al., 2004; Oka et al., 2007). Interestingly, the first step is the dehydration of UDP-Glc to 4-keto-3-deoxy Glc, a similar step to that proposed for the dehydration of rhamnosylisoorientin to maysin by *SM1*. Furthermore, GRMZM2G031311 is located in the mapping region of *SM1*, suggesting its possible involvement in this reaction (McMullen et al., 2004).

P1 Regulates the Expression of Several Transcription Factor Genes

Although the vast majority of the 3000 to 4000 maize genes encoding transcription factors (Yilmaz et al., 2009) are not affected in silks or pericarps by the expression of *P1*, our results show that *P1* can directly control the expression of several regulatory genes (see Supplemental Figure 4 online). While no regulatory gene is shared between the three samples, three are present in both 14- and 25-DAP pericarps. These correspond to GRMZM2G137541 (bHLH151) and GRMZM2G051528 (MYB95), both of which are activated in 14-DAP and repressed in 25-DAP pericarps, and GRMZM2G012654 (CADR16), which is repressed by P1 in both pericarp developmental time points. *MYB95*, encoding an R2R3-MYB transcription factor with high identity with P1 in the MYB domain and resulting from a grass-specific amplification of a particular subclass of R2R3-MYB genes (Dias et al., 2003) was previously implicated in the control of phenylpropanoids (Dias and Grotewold, 2003). These results suggest that *P1* not only directly activates enzymes of the flavonoid/phenylpropanoid pathway but also controls transcription factors that are in turn regulating various aspects of plant metabolism. These results are perhaps more consistent with the maize gene regulatory network being democratic, with the information flow more distributed and a less obvious distinction between regulatory layers, as would be the case in a autocratic hierarchical organization (Yu and Gerstein, 2006; Jothi et al., 2009). Of course, precisely understanding how P1 fits within the maize gene regulatory network will need to await similar studies being conducted on other transcription factors.

Conclusions

A key step in establishing plant gene regulatory networks is the identification of the genes that transcription factors bind and regulate in vivo. Gene regulatory networks have often been considered as having a hierarchical topology, with transcription factors functioning in the center levels being most highly connected (Yu and Gerstein, 2006; Bhardwaj et al., 2010). One type of connectivity is the number of other genes that a transcription factor controls. Given that higher connectivity is, at least in the *Escherichia coli* and yeast gene regulatory networks, associated with more essential functions, one would presume that the regulator of a specialized metabolic pathway, such as P1, which directly controls genes encoding biosynthetic enzymes, would be sparsely connected. Our results derived from combining RNA-Seq and ChIP-Seq experiments in tissues with contrasting *P1* genotypes suggest that this is not the case. Even a transcription factor like P1, functioning in the lowest tier of the maize gene regulatory network, binds hundreds, if not thousands, of genes including other transcriptional regulators. Such results are more consistent with Continuous Network models, where transcription factors bind to all or to a large fraction of all the genes in an organism in a "quantitative continuum of occupancy levels" (Biggin, 2011). Our results also highlight the power of RNA-Seq by itself, or in combination with ChIP-Seq, to identify missing metabolic pathway genes. This study focused on the characterization of F2H1 as a key step in the formation of insecticidal flavones, but other identified *P1*-controlled genes will certainly continue to fill gaps in the maize metabolic grid.

METHODS

Maize Stocks and Plant Materials

The *P1-rr* stock designated as 65-CFS-305 (Brink and Styles, 1966) was obtained from the National Seed Storage Laboratory, Fort Collins, CO. Plant tissues from the B73 maize (*Zea mays*) inbred line were obtained from Instituto Nacional de Tecnologia Agropecuaria Pergamino (Argentina). Near isogenic lines containing *P1-rr* and *P1-ww* were generated by six backcross generations of 65-CFS-305 with A619 (*P1-ww*) followed by three selfing generations to confirm homozygosity. The original 65-CFS-305 line has both *P1-rr* and the *P2* gene in the 4 County 63 background, while the inbred line A619 has a nonfunctional *P1* locus (*P1-ww*) and lacks *P2* (Szalma et al., 2005). The introgressed region from 65-CFS-305 in A619 was determined to extend on chromosome 1 from 35 to 66 Mb (AGPv2) by mapping with Illumina Maize SNP50 array (Ganal et al., 2011). The final near isogenic line also contained a second, nontarget introgressed region of chromosome 6 from 89 to 102 Mb. Pericarps were peeled from 14- and 25-DAP maize ears avoiding any aleurone tissue, and silks were collected 2 to 3 d postemergence, from ears shoots that had been bagged to prevent pollination.

Immunoblot Analyses

We confirmed that the P1 antibody (αP1[344]) previously used for ChIP (Ferreyra et al., 2010) recognized P1 by immunoblot analysis (see Supplemental Figure 8 online). Nuclear proteins were extracted from pericarps using the plant nuclei isolation/extraction kit (Sigma-Aldrich) according to the manufacturer's instructions. Electrophoresis on SDS-PAGE was performed for 40 µg of nuclear proteins, followed by blotting to polyvinylidene fluoride membrane. Membranes were incubated with P1 antibody diluted 1:1000 (in 5% BSA) for 1 h at room temperature. After three to five washes in TBST (50 mM Tris-HCl, pH 8.0, 150 mM NaCl, and 0.1% Tween 20), signal detection was performed using SuperSignal West Femto Chemiluminescent Substrate (Pierce).

ChIP and ChIP-Seq

ChIP was performed by methods previously described (Morohashi and Grotewold, 2009; Morohashi et al., 2009; Ferreyra et al., 2010), with modifications to accommodate for the high concentration of flavonoids present in *P1-rr* pericarps. Briefly, 0.3 g of dissected pericarps were fixed in Buffer A (0.4 M Suc, 10 mM Tris-HCl, pH 8.0, 1 mM EDTA, 1 mM phenylmethylsulfonyl fluoride, and 0.1% formaldehyde) for 10 min under vacuum conditions. Gly was added to a final concentration of 0.1 M, and incubation was continued for an additional 5 min. Fixed pericarps were washed in distilled water and frozen in liquid N_2. The tissue was ground in liquid N_2, followed by nuclear isolation using the plant nuclei isolation/extraction kit according to the manufacturer's instructions (Sigma-Aldrich). Nuclear-enriched extracts were resuspended in 100 μL lysis buffer (50 mM HEPES, pH 7.5, 150 mM NaCl, 1 mM EDTA, 1% Triton X-100, 0.1% deoxycholate, 0.1% SDS, 1 mM phenylmethylsulfonyl fluoride, and 10 mM sodium butyrate) and plant proteinase inhibitor cocktail (Sigma-Aldrich), followed by sonication with a Bioruptor (Diangenode) to ~300 bp of average fragment size, estimated by agarose electrophoresis.

For quantitative (real-time) PCR analyses of ChIPed materials, to correct for PCR bias, 1 pg of pUC19 plasmid was spiked into input and immunoprecipitated (ChIP) DNA. Quantitative PCR was performed using 0.1 to 1 μL of input or ChIPed DNA with Buffer J of the FailSafe PCR system (Epicentre Biotechnologies). ChIP-Seq library preparation was performed according to Quail's method (Quail et al., 2008). ChIP DNA were subjected to end repair and A-base addition, followed by ligation with custom adapters. Barcode sequences of each adapter correspond to the following: AGGCC, ChIP of *P1-ww* at 14 DAP; AACCA, AGAAG, ChIP of *P1-rr* at 14 DAP. Illumina GA sequencing with SR30 and SR45 was performed by the OSUCCC Nucleic Acid Shared Resource-Illumina GAII Core and the OARDC Molecular and Cellular Imaging Center (The Ohio State University).

We defined target genes as those that contain ChIP-Seq peaks located within transcribed regions of genes, in introns or 5 kb upstream of the TSS or 5 kb downstream of the site of polyadenylation.

mRNA-Seq Library Preparation

Total RNA (2 μg) extracted from *P1-rr* and *P1-ww* pericarps harvested at 14 and 25 DAP and silks harvested 1 to 2 d postemergence were used. The preparation of mRNA-Seq libraries was performed according to instructions from the Illumina mRNA-Seq sample preparation kit (RS-100-0801 Illumina). Total RNA extracted from *P1-rr* and *P1-ww* pericarps harvested at 14 and 25 DAP and silks harvested 1 to 2 d postemergence were treated with DNaseI (Promega) twice to ensure no genomic DNA contamination. Two micrograms of total RNA was subjected to two rounds of hybridization to oligo(dT) beads (Illumina). The poly(A)-enriched mRNA was fragmented by heating at 94°C for 5 min in fragmentation buffer supplied by Illumina, followed by ethanol precipitation. The fragmented mRNA was added to 1$\times$ first-strand buffer (2.5 mM deoxynucleotide triphosphate, 10 mM DTT, RNaseOUT, and random primers mix). After adding Superscript II, first-strand cDNA synthesis was performed at 25°C for 10 min, 42°C for 50 min, and 70°C for 15 min. The second-strand cDNA synthesis was performed in GEX Second Strand Buffer (25 mM deoxynucleotide triphosphate, 1 μL RNase H, and 5 μL DNA Pol I for 2.5 h at 16°C) and purified by a PCR purification kit (Qiagen). After end repair and A-base addition, adapter ligation was performed using custom made adapters or Illumina multiplexing system. For custom-made adapters, reverse oligo-adapters consisting of SLX-R_P1 and SLX-R_P2 and forward oligo adapters consisting of SLX-N_P1 and SLX-N_P2, where underlined nucleotides (see Supplemental Table 4 online) correspond to a barcode sequence, which was either AATCG, AACAC, AACGT, or AACTG in *P1-ww* at 14 or 25 DAP and *P1-rr* 14 or 25 DAP, respectively. For using Illumina multiplexing system, the overall procedure

was performed according to the manufacturer's instructions (MultiplexPE_SamplePrep_1005361_RevB). We used Index 1 (ATCACG) or 2 (CGATGT) for *P1-rr* or *P1-ww* silk, respectively. For both procedures, ligated fragments were subjected to electrophoresis for selection of fragments of ~300 bp in length, followed by PCR amplification (20 cycles). PCR products were purified with Agencourt AMPure (Beckman Coulter). Library DNA was checked for concentration and size distribution in an Agilent Bioanalyzer before being subjected to Illumina GA sequencing with SR30 (for pericarp) and SR72 (for silk) using the OSUCCC Nucleic Acid Shared Resource-Illumina GAII Core and the OARDC Molecular and Cellular Imaging Center (The Ohio State University). For the Illumina multiplexing system, the overall procedure was according to the manufacturer's instructions (MultiplexPE_SamplePrep_1005361_RevB).

High-Throughput DNA-Sequence Analysis and Computational Analyses

K-means clustering was performed with the K-means/K-medians clustering embedded in the MEV program (http://www.tm4.org/mev). The number of clusters (8) was defined by the Figures of Merit application. Ratios of FPKM of *P1-rr/P1-ww* in 14- and 25-DAP pericarp and silk were transformed to $\log_2$ values, which were subjected to K-means clustering using the default Euclidian distance. Peak distributions of P1 ChIP-Seq were calculated based on MACS output using both BEDTools (http://code.google.com/p/bedtools/) and custom-made Perl scripts.

ChIP-Seq reads were aligned to the maize genome (release 5b.60) using Bowtie (Langmead et al., 2009). We ran Bowtie version 0.11.3 allowing three mismatches per read and reporting only unique alignments (-v 3 -m 1–best –strata). ChIP-Seq peaks were detected by MACS (Zhang et al., 2008; Feng et al., 2011). We used MACS14 version 1.4.0 beta, and duplicates were allowed (–keepdup) and P value < 0.0001 (-p 1e-4). RNA-Seq reads were aligned against maize genome with Splice Junction Mapper TopHat software (Trapnell et al., 2009), and transcript levels were calculated as FPKM with Cufflinks (Trapnell et al., 2010). We used gene models belonging to the maize genome filtered gene set for transcript abundance calculation. We applied a negative binomial model distribution model (P value < 0.05) considering nonaligned reads and reads that align to the genome but not to genes to calculate the threshold FPKM to consider the minimal significant expression for each transcript. We used the Cuffdiff tool in TopHat to estimate differentially expressed gene models. Cuffdiff uses the beta negative binomial to account for overdispersed data.

Gene Expression Analyses by qRT-PCR

Three independent biological replicates (i.e., materials obtained from different plants) from *P1-rr* and *P1-ww* pericarp and silk samples were snap-frozen in $N_2(l)$ and stored at −80°C. Total RNA was extracted using the RNeasy plant mini kit followed by DNaseI treatment (Qiagen). cDNA was synthesized from 1 μg of total RNA using SuperScript Reverse Transcriptase II (Invitrogen) with oligo-dT$_{12-18}$ as primer. The resulting cDNA was used as template for qRT-PCR amplification in an iCycler iQ detection system with Optical System Software (v3.0a; Bio-Rad) using the intercalation dye SYBR Green I (Invitrogen) as a fluorescent reporter and Platinum Taq Polymerase (Invitrogen). Primers were designed to generate fragments between 80 and 150 bp using Primer3 (Rozen and Skaletsky, 2000). Three biological replicates were performed for each sample, in addition to negative controls without reverse transcriptase. Actin was used to normalize the values obtained. Amplification conditions were as follows: 2 min denaturation at 94°C; 40 to 45 cycles of 94°C for 15 s, 57°C for 20 s, and 72°C for 20 s, followed by a final extension step at 72°C for 5 min.

Cloning and Expression of *F2H1*

A full-length cDNA corresponding to GRMZM2G167336 was amplified by PCR using the primers ZmFNS1-BamHI-forward and ZmFNS1-EcoRI-reverse harboring the *Bam*HI and *Eco*RI restriction sites, respectively, for further cloning. PCR was performed with GoTaq Polymerase (Promega) using the FailSafe PCR System (Epicentre Biotechnologies) under the following conditions: $1\times$ Premix G, 0.5 μM of each primer, and cDNA from *P1-rr* pericarps in 25 μL of final volume. Amplification conditions were as follows: 95°C for 30 s, 30 s annealing at 58°C, 130-s extension at 72°C, by 35 cycles. Primers for cDNA were designed based on the sequence provided by the maize genome sequence (release 5b60 at http://www.maizesequence.org, GRMZM2G167336). The PCR product was purified from the gels, digested with the corresponding restriction enzymes, purified, and cloned into pGZ25, generating the plasmid pGZ25-ZmF2H. the pGZ25 vector corresponds to a modified version of plasmid YEplac112 (Gietz and Sugino, 1988) in which the glyceraldehyde 3-phosphate dehydrogenase promoter was inserted at the *Hin*dIII site.

Flavonoid Analyses

The pGZ25-ZmF2H plasmid and pGZ25 empty vector were transformed into competent WAT11 (Urban et al., 1997) yeast cells (kindly provided by P. Urban) by electroporation. Yeast colonies harboring the plasmids were selected by growth on synthetic complete media agar plates lacking uracil and Trp (synthetic complete media Ura- Trp-). For in vivo yeast assays, an individual recombinant yeast colony was grown overnight at 30°C in 5 mL liquid SC Ura- Trp- medium containing 2% (w/v) Glc. After incubation to $OD_{600} = 1.0$, an aliquot of this culture was collected by centrifugation, washed in sterile water, and used to seed the 10 mL induction medium, SC Ura- Trp- containing 2% (w/v) Gal. The substrates naringenin or eriodictyol were then added to a final concentration of 0.35 mM. After incubation for 16 to 20 h at 30°C, 750 μL culture aliquots were extracted with equal volume of ethyl acetate, vacuum dried, and resuspended in 80% methanol for subsequent HPLC analysis. HPLC analyses were performed with ÄKTA basic 10/100 (Amersham Biosciences), using a Phenomenex LUNA C18 column (150 mm $\times$ 4.6 mm, 5 μm). Data were collected and analyzed using the UNICORN control system program (version 3.0). Compound separation was by linear gradient elution from 20% methanol:80% 10 mM ammonium acetate, pH 5.6, to 100% methanol at a flow rate of 0.75 mL min^{-1}. Absorbance units were detected at 268, 292, and 340 nm using a UV900 detector (Amersham Biosciences). Retention times of the products analyzed were compared with those of authentic commercial standards (Sigma-Aldrich).

Synthesis of 2-Hydroxynaringenin

2-Hydroxynaringenin was synthesized according to the published method (Britsch, 1990). Apigenin (54 mg) was dissolved in freshly distilled pyridine (27 mL) and water (0.27 mL) containing potassium hydroxide powdered in anhydrous diethyl ether (6.48 g). The reaction mixture was refluxed for 2 h, and the pyridine was evaporated at reduced pressure in a rotary evaporator at 40°C. Water (25 mL) was added in an ice bath, and the pH was adjusted to 5.0 with acetic acid. The product was extracted with ethyl acetate (3×25 mL) and, after the addition of water (0.5 mL), the organic solvent was evaporated under reduced pressure at room temperature. Methanol (0.5 mL) was added to the aqueous residue and the crude reaction mixture was chromatographed in a Sephadex LH 201000 column equilibrated with methanol/water 80:20 and eluted with the same solvent mixture. Fractions were analyzed by thin layer chromatography and concentrated to yield 5 mg (9%) of 2-hydroxynaringenin. Thin layer chromatography was performed using commercial silica gel plates (Merck Silica Gel 60 F254) and visualized with UV light and a *p*-anysaldehyde solution (2.5 mL of *p*-anysaldehyde + 2.5 mL of H_2SO_4 + 0.25 mL of AcOH + 95 mL of ethanol). The ^{1}H NMR spectrum was in agreement with that described in the literature for the desired product (Britsch, 1990) and

also evidenced the presence of some apigenin, probably formed by dehydration of 2-hydroxynaringenin upon drying. LC-MS confirmed that both products were present in the mixture. NMR spectra were recorded at 300 MHz for ^{1}H on a Bruker Avance-300 DPX spectrometer with $(CH3)_4Si$ as internal standard, resulting in the following: ^{1}H NMR (300 MHz; acetone-d_6) δ: 7.62 (br s, 2 H, H-2′ and H-6′), 6.89 (δ, $J = 8.4$ Hz, 2 H, H-3′ and H-5′), 5.97 (s, 2 H, H-6 and H-8). Chemical shifts are reported in delta (δ) units in ppm, and splitting patterns are designated as s, singlet; d, doublet; and br, broad.

Gene Model Verification of Phenylpropanoid Biosynthetic Genes

Maize gene models with high homology to known phenylpropanoid pathway members and with strong support from literature and bioinformatic searches were verified by a multitiered approach. The maize gene model names (GRMZMs) were searched on both the maize sequence website (http://maizesequence.org/index.html) and the maize genome database (http://www.maizegdb.org/) for evidence of gene expression. Next, cDNA sequences from the gene models were BLASTn compared with *Arabidopsis thaliana* sequences to confirm their initial annotations. Each gene model was then compared against available maize RNA-Seq data sets to determine their relative expression levels in various maize tissues. Models that had strong evidence of expression and appeared to match gene annotations of *Arabidopsis* genes were added to the final list seen in Supplemental Data Set 2 online.

Transient Expression Assays Using Maize Leaf Protoplasts

Protoplasts from 11- to 13-d-old etiolated maize seedlings were obtained from kernels of B73xMo17 plants. After chopping second or third leaves into small pieces, leaf stripes were digested in 3% cellulase RS, 0.6% macerozyme R10 (both from Yakult Honsha Co.), 0.6 M mannitol, 10 mM MES, pH 5.7, 5 mM $CaCl_2$, and 0.1% (w/v) BSA for 15 min under vacuum followed by 2:30 h gentle shaking (40 rpm) at 25°C in the dark. After releasing the protoplasts at 80*g* (90 rpm), the protoplasts were filtered through a 35-μm nylon mesh and collected by centrifugation at 150*g* for 1 min. The protoplasts were washed in ES buffer (0.6 M mannitol, 5 mM MES, pH 5.7, and 10 mM KCl) and counted with a hemocytometer. Electroporation was performed on ~100,000 protoplasts with 40 μg of total DNA per transformation, using 100 V/cm, 10 ms, and one pulse with a BTX Electro-Square-Porator T820. After electroporation, protoplasts were incubated for 18 to 22 h in the dark at room temperature before performing the luciferase reaction. Transformation efficiency was estimated following green fluorescent protein expression.

When performing the transient expression analysis on protoplasts, we noticed that the high Renilla values (derived from cotransformation with pUbi::Renilla and used as a transformation normalization control) in the transformation without transcription factor dropped considerably (from ~1.4 $\times$ 10^6 light units without the transcription factor to 3 to 5 $\times$ 10^5 light units when P1 or C1+R were included) when the transcription factors P1 or C1+R were included. While these effects were most noticeable on pA1*::Luc, we observed them also on the other pathway promoters (see Supplemental Figure 6 online). However, this tendency was not observed when ZmMYB40 or ZmMYB31, an activator and a repressor or phenylpropanoid biosynthesis respectively, were used.

Electrophoretic Mobility Shift Assay

Electrophoretic mobility shift assay was performed essentially as described (Chai et al., 2011). The ZmP1 MYB domain (*Zm*P1^{MYB}) fusion with N-terminal poly-His was expressed in *Escherichia coli* and affinity purified using nickel-nitrilotriacetic acid beads under natural conditions (Williams and Grotewold, 1997). The promoter fragments of *rhm* and *whp* used as probes for electrophoretic mobility shift assay were generated by PCR using primer pairs in Supplemental Table 4 online, in which one of

the primers was radioactively labeled with [γ-³²P]ATP using T4-polynucleotide kinase. The radioactively labeled DNA fragments were then purified and quantified. Ten nanograms of purified P1^{MYB} was incubated with equal molar of probes (with radioactivity ~10⁵ cpm) for 30 min, and the P1^{MYB}-probe complexes were separated by PAGE. After PAGE, the gel was dried onto Whatman paper and then subjected to autoradiography at −70°C.

Accession Numbers

All the short sequence data generated as part of this study have been deposited in the Gene Expression Omnibus (http://www.ncbi.nlm.nih.gov/geo/) under accession numbers GSE38413, GSE38414 for RNA-Seq, and GSE38587 for ChIP-Seq.

Supplemental Data

The following materials are available in the online version of this article.

Supplemental Figure 1. *P1-rr* and *P1-ww* Pericarps at Different Developmental Stages.

Supplemental Figure 2. qRT-PCR Validation of Genes Identified as Upregulated in *P1-rr* by RNA-Seq.

Supplemental Figure 3. Global Gene Expression Analysis from RNA-Seq Experiments Conducted from Root, Shoot, Leaf, Silk, and Pericarp Tissues.

Supplemental Figure 4. Control of the Expression of Transcription Factor Genes by *P1*.

Supplemental Figure 5. Box Plots Corresponding to Expression Distribution within the K1 to K8 Clusters.

Supplemental Figure 6. Control of Flavonoid Biosynthetic Genes by *P1*.

Supplemental Figure 7. LC-MS Analysis of ZmF2H1 Activity Products and Phylogenetic Analyses of Amino Acid Sequences of Cytochrome P450 Enzymes.

Supplemental Figure 8. P1 Protein Expression Is Highest in *P1-rr* 14-DAP Pericarps.

Supplemental Figure 9. Validation of P1 ChIP-Seq Results by ChIP-PCR and ChIP-qPCR.

Supplemental Figure 10. Motif Enrichment in Genome-Wide Location Analysis Peaks in *P1*-Controlled Genes.

Supplemental Figure 11. Venn Diagrams Summarizing the Overlap between the Genes Expressed in Pericarp and Silks as Detected with RNA-Seq and Microarrays.

Supplemental Figure 12. Phylogenetic Analyses of UDP-Sugar: Glycosyltransferases from Higher Plants.

Supplemental Figure 13. P1 Binds in Vivo to *F2H1* and *CYP98A*.

Supplemental Table 1. Summary of RNA-Seq Reads Obtained per Tissue Analyzed.

Supplemental Table 2. Summary of ChIP-Seq Reads Obtained in P1-rr versus P1-ww Pericarps at 14 DAP.

Supplemental Table 3. Percentage of Peaks Present in ChIP-Seq Experiments.

Supplemental Table 4. Primers Used in This Study.

Supplemental Data Set 1. Genome-Wide Analysis of Gene Expression in Maize Tissues.

Supplemental Data Set 2. Phenylpropanoid Genes Analyzed in RNA-Seq Experiments.

Supplemental Data Set 3. Text File of the Alignment Corresponding to the Phylogenetic Analysis in Supplemental Figure 12.

Supplemental Data Set 4. Text File of the Alignment Corresponding to the Phylogenetic Analysis in Supplemental Figure 7.

AUTHOR CONTRIBUTIONS

K.M. and E.G. were primary designers of the research. K.M., M.I.C., L.F.F., M.K.M.-G., L.P., A.Y., A.F., B.C., J.E., E.R., and S.P. performed different aspects of the research. M.M. contributed genetic material and together with E.G. and P.C. contributed to the analysis of the data. K.M., M.I.C., M.K.M.-G., and E.G. wrote the article.

REFERENCES

Anderson, E.G. (1924). Pericarp studies in maize II: The allelomorphism of a series of factors for pericarp color. Genetics **9:** 442–453.

Anderson, E.G., and Emerson, R.A. (1923). Pericarp studies in maize. I: The inheritance of pericarp colors. Genetics **8:** 466–476.

Bate-Smith, E.C. (1969). Luteoforol (3′,4,4′5,7,-Pentahydroxyflavan in *Sorghum vulgare* L. Phytochemistry **8:** 1803–1810.

Bernhardt, J., Stich, K., Schwarz-Sommer, Z., Saedler, H., and Wienand, U. (1998). Molecular analysis of a second functional *A1* gene (*dihydroflavonol 4-reductase*) in *Zea mays*. Plant J. **14:** 483–488.

Bhardwaj, N., Yan, K.K., and Gerstein, M.B. (2010). Analysis of diverse regulatory networks in a hierarchical context shows consistent tendencies for collaboration in the middle levels. Proc. Natl. Acad. Sci. USA **107:** 6841–6846.

Biggin, M.D. (2011). Animal transcription networks as highly connected, quantitative continua. Dev. Cell **21:** 611–626.

Bily, A.C., Reid, L.M., Taylor, J.H., Johnston, D., Malouin, C., Burt, A.J., Bakan, B., Regnault-Roger, C., Pauls, K.P., Arnason, J.T., and Philogène, B.J. (2003). Dehydrodimers of ferulic acid in maize grain pericarp and aleurone: Resistance factors to fusarium graminearum. Phytopathology **93:** 712–719.

Birney, E., et al, ENCODE Project Consortium (2007). Identification and analysis of functional elements in 1% of the human genome by the ENCODE pilot project. Nature **447:** 799–816.

Bodeau, J.P., and Walbot, V. (1992). Regulated transcription of the maize *Bronze-2* promoter in electroporated protoplasts requires the *C1* and *R* gene products. Mol. Gen. Genet. **233:** 379–387.

Brazier-Hicks, M., Evans, K.M., Gershater, M.C., Puschmann, H., Steel, P.G., and Edwards, R. (2009). The *C*-glycosylation of flavonoids in cereals. J. Biol. Chem. **284:** 17926–17934.

Brink, R.A., and Styles, D. (1966). A collection of pericarp factors. Maize Genet. Coop. News Lett. **40:** 149–160.

Britsch, L. (1990). Purification and characterization of flavone synthase I, a 2-oxoglutarate-dependent desaturase. Arch. Biochem. Biophys. **282:** 152–160.

Bruce, W., Folkerts, O., Garnaat, C., Crasta, O., Roth, B., and Bowen, B. (2000). Expression profiling of the maize flavonoid pathway genes controlled by estradiol-inducible transcription factors CRC and P. Plant Cell **12:** 65–80.

Buckner, B., Kelson, T.L., and Robertson, D.S. (1990). Cloning of the *y1* locus of maize, a gene involved in the biosynthesis of carotenoids. Plant Cell **2:** 867–876.

Bushman, B.S., Snook, M.E., Gerke, J.P., Szalma, S.J., Berhow, M.A., Houchins, K.E., and McMullen, M.D. (2002). Two loci exert major effects on chlorogenic acid synthesis in maize silks. Crop Sci. **42:** 1669–1678.

Byrne, P.F., Darrah, L.L., Snook, M.E., Wisemen, B.R., Widstrom, N.W., Moellenbeck, D.J., and Barry, B.D. (1996a). Maize silk-browning, maysin content, and antibiosis to the corn earworm, *Helicoverpa zea* (Boddie). Maydica **41:** 13–18.

Byrne, P.F., McMullen, M.D., Snook, M.E., Musket, T.A., Theuri, J.M., Widstrom, N.W., Wiseman, B.R., and Coe, E.H. (1996b). Quantitative trait loci and metabolic pathways: Genetic control of the concentration of maysin, a corn earworm resistance factor, in maize silks. Proc. Natl. Acad. Sci. USA **93:** 8820–8825.

Carr, A., and Biggin, M.D. (1999). A comparison of in vivo and in vitro DNA-binding specificities suggests a new model for homeoprotein DNA binding in *Drosophila* embryos. EMBO J. **18:** 1598–1608.

Chai, C., Xie, Z., and Grotewold, E. (2011). SELEX (Systematic Evolution of Ligands by EXponential Enrichment), as a powerful tool for deciphering the protein-DNA interaction space. Methods Mol. Biol. **754:** 249–258.

Christensen, A.H., and Quail, P.H. (1996). Ubiquitin promoter-based vectors for high-level expression of selectable and/or screenable marker genes in monocotyledonous plants. Transgenic Res. **5:** 213–218.

Coe, E.H., Jr. (2001). The origins of maize genetics. Nat. Rev. Genet. **2:** 898–905.

Dias, A.P., Braun, E.L., McMullen, M.D., and Grotewold, E. (2003). Recently duplicated maize *R2R3 Myb* genes provide evidence for distinct mechanisms of evolutionary divergence after duplication. Plant Physiol. **131:** 610–620.

Dias, A.P., and Grotewold, E. (2003). Manipulating the accumulation of phenolics in maize cultured cells using transcription factors. Biochem. Eng. J. **14:** 207–216.

Du, Y., Chu, H., Chu, I.K., and Lo, C. (2010a). CYP93G2 is a flavanone 2-hydroxylase required for *C*-glycosylflavone biosynthesis in rice. Plant Physiol. **154:** 324–333.

Du, Y., Chu, H., Wang, M., Chu, I.K., and Lo, C. (2010b). Identification of flavone phytoalexins and a pathogen-inducible flavone synthase II gene (*SbFNSII*) in sorghum. J. Exp. Bot. **61:** 983–994.

Emerson, R.A. (1911). Genetic correlation and spurious allelomorphism in maize. Ann. Rep. Nebraska Ag. Exp. Station **24:** 59–90.

Emerson, R.A. (1917). Genetical studies of variegated pericarp in maize. Genetics **2:** 1–35.

Eveland, A.L., Satoh-Nagasawa, N., Goldshmidt, A., Meyer, S., Beatty, M., Sakai, H., Ware, D., and Jackson, D. (2010). Digital

gene expression signatures for maize development. Plant Physiol. **154:** 1024–1039.

Ferreyra, M.L., Rius, S., Emiliani, J., Pourcel, L., Feller, A., Morohashi, K., Casati, P., and Grotewold, E. (2010). Cloning and characterization of a UV-B-inducible maize flavonol synthase. Plant J. **62:** 77–91.

Feng, J., Liu, T., and Zhang, Y. (2011). Using MACS to identify peaks from ChIP-Seq data. Curr. Protoc. Bioinformatics 2011 Jun; Chapter 2: Unit 2.14.

Fliegmann, J., Furtwängler, K., Malterer, G., Cantarello, C., Schüler, G., Ebel, J., and Mithöfer, A. (2010). Flavone synthase II (*CYP93B16*) from soybean (*Glycine max* L.). Phytochemistry **71:** 508–514.

Flintham, J.E. (2000). Different genetic components control coat-imposed and embryo-imposed dormancy in wheat. Seed Sci. Res. **10:** 43–50.

Franken, P., Niesbach-Klösgen, U., Weydemann, U., Maréchal-Drouard, L., Saedler, H., and Wienand, U. (1991). The duplicated chalcone synthase genes *C2* and *Whp* (*white pollen*) of *Zea mays* are independently regulated; evidence for translational control of *Whp* expression by the anthocyanin intensifying gene *in*. EMBO J. **10:** 2605–2612.

Ganal, M.W., et al (2011). A large maize (*Zea mays* L.) SNP genotyping array: Development and germplasm genotyping, and genetic mapping to compare with the B73 reference genome. PLoS ONE **6:** e28334.

Garcia-Lara, S., Bergvinson, D.J., Burt, A.J., Ramputh, A.I., Diaz-Pontones, D.M., and Arnason, J.T. (2004). The role of pericarp cell wall components in maize weevil resistance. Crop Sci. **44:** 1546–1552.

Gietz, R.D., and Sugino, A. (1988). New yeast-*Escherichia coli* shuttle vectors constructed with *in vitro* mutagenized yeast genes lacking six-base pair restriction sites. Gene **74:** 527–534.

Goff, S.A., Klein, T.M., Roth, B.A., Fromm, M.E., Cone, K.C., Radicella, J.P., and Chandler, V.L. (1990). Transactivation of anthocyanin biosynthetic genes following transfer of *B* regulatory genes into maize tissues. EMBO J. **9:** 2517–2522.

Goodman, C.D., Casati, P., and Walbot, V. (2004). A multidrug resistance-associated protein involved in anthocyanin transport in *Zea mays*. Plant Cell **16:** 1812–1826.

Grotewold, E. (2006). The genetics and biochemistry of floral pigments. Annu. Rev. Plant Biol. **57:** 761–780.

Grotewold, E., Athma, P., and Peterson, T. (1991a). A possible hot spot for *Ac* insertion in the maize *P* gene. Mol. Gen. Genet. **230:** 329–331.

Grotewold, E., Athma, P., and Peterson, T. (1991b). Alternatively spliced products of the maize *P* gene encode proteins with homology to the DNA-binding domain of myb-like transcription factors. Proc. Natl. Acad. Sci. USA **88:** 4587–4591.

Grotewold, E., Chamberlin, M., Snook, M., Siame, B., Butler, L., Swenson, J., Maddock, S., St Clair, G., and Bowen, B. (1998). Engineering secondary metabolism in maize cells by ectopic expression of transcription factors. Plant Cell **10:** 721–740.

Grotewold, E., Drummond, B.J., Bowen, B., and Peterson, T. (1994). The myb-homologous *P* gene controls phlobaphene pigmentation in maize floral organs by directly activating a flavonoid biosynthetic gene subset. Cell **76:** 543–553.

Hernandez, J.M., Heine, G.F., Irani, N.G., Feller, A., Kim, M.-G., Matulnik, T., Chandler, V.L., and Grotewold, E. (2004). Different mechanisms participate in the R-dependent activity of the R2R3 MYB transcription factor C1. J. Biol. Chem. **279:** 48205–48213.

Huang, B.Q., and Sheridan, W.F. (1994). Female gametophyte development in maize: Microtubular organization and embryo sac polarity. Plant Cell **6:** 845–861.

Jothi, R., Balaji, S., Wuster, A., Grochow, J.A., Gsponer, J., Przytycka, T.M., Aravind, L., and Babu, M.M. (2009). Genomic analysis reveals a tight link between transcription factor dynamics and regulatory network architecture. Mol. Syst. Biol. **5:** 294.

Kaufmann, K., Muiño, J.M., Jauregui, R., Airoldi, C.A., Smaczniak, C., Krajewski, P., and Angenent, G.C. (2009). Target genes of the MADS transcription factor SEPALLATA3: Integration of developmental and hormonal pathways in the *Arabidopsis* flower. PLoS Biol. **7:** e1000090.

Kaufmann, K., Wellmer, F., Muiño, J.M., Ferrier, T., Wuest, S.E., Kumar, V., Serrano-Mislata, A., Madueño, F., Krajewski, P., Meyerowitz, E.M., Angenent, G.C., and Riechmann, J.L. (2010). Orchestration of floral initiation by APETALA1. Science **328:** 85–89.

Kiesselbach, T.A. (1980). The Structure and Reproduction of Corn. (Lincoln, NE: University of Nebraska Press).

Langmead, B., Trapnell, C., Pop, M., and Salzberg, S.L. (2009). Ultrafast and memory-efficient alignment of short DNA sequences to the human genome. Genome Biol. **10:** R25.

Lechelt, C., Peterson, T., Laird, A., Chen, J., Dellaporta, S.L., Dennis, E., Peacock, W.J., and Starlinger, P. (1989). Isolation and molecular analysis of the maize P locus. Mol. Gen. Genet. **219:** 225–234.

Lee, J., He, K., Stolc, V., Lee, H., Figueroa, P., Gao, Y., Tongprasit, W., Zhao, H., Lee, I., and Deng, X.W. (2007). Analysis of transcription factor HY5 genomic binding sites revealed its hierarchical role in light regulation of development. Plant Cell **19:** 731–749.

Lefrançois, P., Euskirchen, G.M., Auerbach, R.K., Rozowsky, J., Gibson, T., Yellman, C.M., Gerstein, M., and Snyder, M. (2009). Efficient yeast ChIP-Seq using multiplex short-read DNA sequencing. BMC Genomics **10:** 37.

Machanick, P., and Bailey, T.L. (2011). MEME-ChIP: Motif analysis of large DNA datasets. Bioinformatics **27:** 1696–1697.

Martens, S., and Mithöfer, A. (2005). Flavones and flavone synthases. Phytochemistry **66:** 2399–2407.

McClintock, B. (1949). Mutable loci in maize. Year B. Carnegie Inst. Wash. **48:** 142–154.

McClintock, B. (1950). The origin and behavior of mutable loci in maize. Proc. Natl. Acad. Sci. USA **36:** 344–355.

McMullen, M.D., Kross, H., Snook, M.E., Cortés-Cruz, M., Houchins, K.E., Musket, T.A., and Coe, E.H. Jr. (2004). Salmon silk genes contribute to the elucidation of the flavone pathway in maize (*Zea mays* L.). J. Hered. **95:** 225–233.

McMullen, M.D., Snook, M., Lee, E.A., Byrne, P.F., Kross, H., Musket, T.A., Houchins, K., and Coe, E.H. Jr. (2001). The biological basis of epistasis between quantitative trait loci for flavone and 3-deoxyanthocyanin synthesis in maize (*Zea mays* L.). Genome **44:** 667–676.

Mehrtens, F., Kranz, H., Bednarek, P., and Weisshaar, B. (2005). The Arabidopsis transcription factor MYB12 is a flavonol-specific regulator of phenylpropanoid biosynthesis. Plant Physiol. **138:** 1083–1096.

Mendel, G. (1950). Gregor Mendel's letters to Carl Nägeli, 1866-1873. Genetics **35:** 1–29.

Meyer, J.D., Snook, M.E., Houchins, K.E., Rector, B.G., Widstrom, N.W., and McMullen, M.D. (2007). Quantitative trait loci for maysin synthesis in maize (*Zea mays* L.) lines selected for high silk maysin content. Theor. Appl. Genet. **115:** 119–128.

Meyers, M.T. (1927). A second recessive factor for brown pericarp in maize. Ohio J. Sci. **27:** 295–300.

Moreno-Risueno, M.A., Busch, W., and Benfey, P.N. (2010). Omics meet networks—Using systems approaches to infer regulatory networks in plants. Curr. Opin. Plant Biol. **13:** 126–131.

Morohashi, K., and Grotewold, E. (2009). A systems approach reveals regulatory circuitry for *Arabidopsis* trichome initiation by the GL3 and GL1 selectors. PLoS Genet. **5:** e1000396.

Morohashi, K., Xie, Z., and Grotewold, E. (2009). Gene-specific and genome-wide ChIP approaches to study plant transcriptional networks. Methods Mol. Biol. **553:** 3–12.

Niu, W., et al. (2011). Diverse transcription factor binding features revealed by genome-wide ChIP-seq in *C. elegans*. Genome Res. **21:** 245–254.

Oka, T., Nemoto, T., and Jigami, Y. (2007). Functional analysis of *Arabidopsis thaliana* RHM2/MUM4, a multidomain protein involved in UDP-D-glucose to UDP-L-rhamnose conversion. J. Biol. Chem. **282:** 5389–5403.

Ordas, B., Malvar, R.A., Santiago, R., and Butron, A. (2010). QTL mapping for Mediterranean corn borer resistance in European flint germplasm using recombinant inbred lines. BMC Genomics **11:** 174.

Penning, B.W., et al. (2009). Genetic resources for maize cell wall biology. Plant Physiol. **151:** 1703–1728.

Pompon, D., Louerat, B., Bronine, A., and Urban, P. (1996). Yeast expression of animal and plant P450s in optimized redox environments. Methods Enzymol. **272:** 51–64.

Quail, M.A., Kozarewa, I., Smith, F., Scally, A., Stephens, P.J., Durbin, R., Swerdlow, H., and Turner, D.J. (2008). A large genome center's improvements to the Illumina sequencing system. Nat. Methods **5:** 1005–1010.

Rabinovich, A., Jin, V.X., Rabinovich, R., Xu, X., and Farnham, P.J. (2008). E2F in vivo binding specificity: Comparison of consensus versus nonconsensus binding sites. Genome Res. **18:** 1763–1777.

Rabinowicz, P.D., Braun, E.L., Wolfe, A.D., Bowen, B., and Grotewold, E. (1999). Maize R2R3 Myb genes: Sequence analysis reveals amplification in the higher plants. Genetics **153:** 427–444.

Roth, B.A., Goff, S.A., Klein, T.M., and Fromm, M.E. (1991). C1- and R-dependent expression of the maize *Bz1* gene requires sequences with homology to mammalian *myb* and *myc* binding sites. Plant Cell **3:** 317–325.

Rozen, S., and Skaletsky, H. (2000). Primer3 on the WWW for general users and for biologist programmers. Methods Mol. Biol. **132:** 365–386.

Sainz, M.B., Grotewold, E., and Chandler, V.L. (1997). Evidence for direct activation of an anthocyanin promoter by the maize C1 protein and comparison of DNA binding by related Myb domain proteins. Plant Cell **9:** 611–625.

Schnable, P.S., et al. (2009). The B73 maize genome: Complexity, diversity, and dynamics. Science **326:** 1112–1115.

Schoch, G., Goepfert, S., Morant, M., Hehn, A., Meyer, D., Ullmann, P., and Werck-Reichhart, D. (2001). CYP98A3 from *Arabidopsis thaliana* is a 3′-hydroxylase of phenolic esters, a missing link in the phenylpropanoid pathway. J. Biol. Chem. **276:** 36566–36574.

Sekhon, R.S., Lin, H., Childs, K.L., Hansey, C.N., Buell, C.R., de Leon, N., and Kaeppler, S.M. (2011). Genome-wide atlas of transcription during maize development. Plant J. **66:** 553–563.

Stracke, R., Ishihara, H., Huep, G., Barsch, A., Mehrtens, F., Niehaus, K., and Weisshaar, B. (2007). Differential regulation of closely related R2R3-MYB transcription factors controls flavonol accumulation in different parts of the *Arabidopsis thaliana* seedling. Plant J. **50:** 660–677.

Styles, E.D., and Ceska, O. (1975). Genetic control of 3-hydroxy- and 3-deoxy-flavonoids in *Zea mays*. Phytochemistry **14:** 413–415.

Styles, E.D., and Ceska, O. (1977). The genetic control of flavonoid synthesis in maize. Can. J. Genet. Cytol. **19:** 289–302.

Styles, E.D., and Ceska, O. (1989). Pericarp flavonoids in genetic strains of *Zea mays*. Maydica **34:** 227–237.

Szalma, S.J., Buckler, E.S., IVSnook, M.E., and McMullen, M.D. (2005). Association analysis of candidate genes for maysin and chlorogenic acid accumulation in maize silks. Theor. Appl. Genet. **110:** 1324–1333.

Tandjung, A.S., Janaswamy, S., Chandrasekaran, R., Aboubacar, A., and Hamaker, B.R. (2005). Role of the pericarp cellulose matrix as a moisture barrier in microwaveable popcorn. Biomacromolecules **6:** 1654–1660.

Tracy, W.F., and Galinat, W.C. (1987). Thickness and cell layer number of the pericarp of sweet corn and some of its relatives. Hort. Sci. **22:** 645–647.

Trapnell, C., Pachter, L., and Salzberg, S.L. (2009). TopHat: Discovering splice junctions with RNA-Seq. Bioinformatics **25:** 1105–1111.

Trapnell, C., Williams, B.A., Pertea, G., Mortazavi, A., Kwan, G., van Baren, M.J., Salzberg, S.L., Wold, B.J., and Pachter, L. (2010). Transcript assembly and quantification by RNA-Seq reveals unannotated transcripts and isoform switching during cell differentiation. Nat. Biotechnol. **28:** 511–515.

Tuerck, J.A., and Fromm, M.E. (1994). Elements of the maize *A1* promoter required for transactivation by the anthocyanin *B/C1* or phlobaphene *P* regulatory genes. Plant Cell **6:** 1655–1663.

Urban, P., Mignotte, C., Kazmaier, M., Delorme, F., and Pompon, D. (1997). Cloning, yeast expression, and characterization of the coupling of two distantly related *Arabidopsis thaliana* NADPH-cytochrome P450 reductases with P450 CYP73A5. J. Biol. Chem. **272:** 19176–19186.

Waiss, A.C., JrChan, B.G., Elliger, C.A., Wiseman, B.R., McMillian, W.W., Widstrom, N.W., Zuber, M.S., and Keaster, A.J. (1979). Maysin, a flavone glycoside from corn silks with antibiotic activity toward corn earworm. J. Econ. Entomol. **72:** 256–258.

Wang, Z., Gerstein, M., and Snyder, M. (2009). RNA-Seq: A revolutionary tool for transcriptomics. Nat. Rev. Genet. **10:** 57–63.

Watt, G., Leoff, C., Harper, A.D., and Bar-Peled, M. (2004). A bifunctional 3,5-epimerase/4-keto reductase for nucleotide-rhamnose synthesis in Arabidopsis. Plant Physiol. **134:** 1337–1346.

Williams, C.E., and Grotewold, E. (1997). Differences between plant and animal Myb domains are fundamental for DNA binding activity, and chimeric Myb domains have novel DNA binding specificities. J. Biol. Chem. **272:** 563–571.

Wiseman, B.R., Snook, M.E., and Isenhour, D.J. (1993). Maysin content and growth of corn earworm larvae (lepidoptera: noctuidae) on silks from first and second ears of corn. J. Econ. Entomol. **86:** 939–944.

Wright, A.D., Moehlenkamp, C.A., Perrot, G.H., Neuffer, M.G., and Cone, K.C. (1992). The maize auxotrophic mutant *orange pericarp* is defective in duplicate genes for tryptophan synthase β. Plant Cell **4:** 711–719.

Xie, Z., Lee, E., Lucas, J.R., Morohashi, K., Li, D., Murray, J.A., Sack, F.D., and Grotewold, E. (2010). Regulation of cell proliferation in the stomatal lineage by the *Arabidopsis* MYB FOUR LIPS via direct targeting of core cell cycle genes. Plant Cell **22:** 2306–2321.

Yang, A., Zhu, Z., Kapranov, P., McKeon, F., Church, G.M., Gingeras, T.R., and Struhl, K. (2006). Relationships between p63 binding, DNA sequence, transcription activity, and biological function in human cells. Mol. Cell **24:** 593–602.

Yilmaz, A., Nishiyama, M.Y., JrFuentes, B.G., Souza, G.M., Janies, D., Gray, J., and Grotewold, E. (2009). GRASSIUS: A platform for comparative regulatory genomics across the grasses. Plant Physiol. **149:** 171–180.

Yu, H., and Gerstein, M. (2006). Genomic analysis of the hierarchical structure of regulatory networks. Proc. Natl. Acad. Sci. USA **103:** 14724–14731.

Zhang, J., Subramanian, S., Zhang, Y., and Yu, O. (2007). Flavone synthases from *Medicago truncatula* are flavanone-2-hydroxylases and are important for nodulation. Plant Physiol. **144:** 741–751.

Zhang, P., Chopra, S., and Peterson, T. (2000). A segmental gene duplication generated differentially expressed myb-homologous genes in maize. Plant Cell **12:** 2311–2322.

Zhang, Y., Liu, T., Meyer, C.A., Eeckhoute, J., Johnson, D.S., Bernstein, B.E., Nusbaum, C., Myers, R.M., Brown, M., Li, W., and Liu, X.S. (2008). Model-based analysis of ChIP-Seq (MACS). Genome Biol. **9:** R137.